NASA TECHNICAL NOTE

NASA TN D-2297

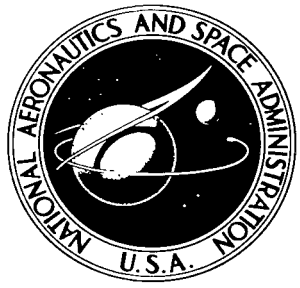

NASA TN D-2297

COMPARISONS OF SOME WING FLUTTER CHARACTERISTICS OBTAINED BY MODIFIED STRIP ANALYSIS, SUBSONIC KERNEL FUNCTION, AND EXPERIMENT

by E. Carson Yates, Jr., and Robert N. Desmarais

Langley Research Center
Langley Station, Hampton, Va.

NATIONAL AERONAUTICS AND SPACE ADMINISTRATION • WASHINGTON, D. C. • MAY 1964

COMPARISONS OF SOME WING FLUTTER CHARACTERISTICS OBTAINED BY MODIFIED STRIP ANALYSIS, SUBSONIC KERNEL FUNCTION, AND EXPERIMENT

By E. Carson Yates, Jr., and Robert N. Desmarais

Langley Research Center
Langley Station, Hampton, Va.

NATIONAL AERONAUTICS AND SPACE ADMINISTRATION

For sale by the Office of Technical Services, Department of Commerce,
Washington, D.C. 20230 -- Price $1.25

COMPARISONS OF SOME WING FLUTTER CHARACTERISTICS OBTAINED BY MODIFIED STRIP ANALYSIS, SUBSONIC KERNEL FUNCTION, AND EXPERIMENT

By E. Carson Yates, Jr., and Robert N. Desmarais
Langley Research Center

SUMMARY

Subsonic flutter characteristics for seven swept and unswept wings have been calculated by the kernel-function method and by a modified strip method. Comparisons of the results from the approximate strip method, from the more rigorous lifting-surface method, and from flutter experiments indicated that all calculated flutter speeds were in good agreement with measured values with the exception of those given by the kernel-function method for two swept wings that had ballast weight distributed along leading or trailing edges. The latter results were unconservative over most of the subsonic range and, within the limits of this investigation, were not significantly improved by changes in the number or type of vibration modes (coupled or uncoupled) nor by increasing the number of downwash collocation points. No appreciable changes were encountered in kernel-function results when uncoupled (rather than coupled) vibration modes were employed for homogeneous wings whose natural modes involved a high degree of bending-torsion coupling.

INTRODUCTION

The intrinsic complexities of rigorous aerodynamic theories for unsteady, three-dimensional, compressible flow have led to extensive use of approximate methods for calculating the oscillatory aerodynamic loads required in flutter analyses. One of these approximate methods is the modified strip analysis[1]

---

[1]In this method, spanwise distributions of steady-flow section lift-curve slope and local aerodynamic center for the undeformed wing are used in conjunction with the "effective" angle-of-attack distribution resulting from the assumed vibration modes in order to obtain values of section lift and pitching moment. The steady-state aerodynamic parameters may be obtained from any suitable theory or experiment, the criterion being that the best method to use is the one that yields the most accurate steady-state load distributions. Circulation functions modified on the basis of loadings for two-dimensional airfoils oscillating in compressible flow are employed to account for the effects of oscillatory motion on the magnitudes and phase angles of the lift and moment vectors.

presented in reference 1 and extended in references 2 to 4. This method, which is limited to relatively low reduced frequencies, has been shown (refs. 1 to 5) to yield subsonic, transonic, and supersonic flutter characteristics that are in generally good agreement with experimental values for a wide variety of wings. In order to investigate further the relative usefulness of this method of flutter analysis, comparisons with the results of other theories as well as with flutter experiments are desirable. References 4 and 6, for example, supply the means for comparing some results of the modified-strip-analysis method with corresponding results obtained from piston theory, from quasi-steady second-order theory, and from flutter experiments for two untapered swept wings at supersonic Mach numbers up to 3.0. Reference 3 includes some comparisons of subsonic results from the modified strip method and from the subsonic kernel-function method (refs. 7 and 8) for a single highly tapered swept wing.

Since the kernel-function method for evaluating the oscillatory aerodynamic loading on a deforming lifting surface is rigorously derived from the linearized equations for unsteady potential flow, it is considered to provide a suitable theoretical criterion for evaluating the approximate modified strip method in the subsonic range. Accordingly, the present report shows comparisons between subsonic flutter results obtained from the modified-strip-analysis method of references 1 to 4, from the subsonic kernel-function method of references 7 and 8, and from flutter experiments (refs. 1 and 9 to 11) for seven swept and unswept wings of moderate aspect ratio. This series of wings involves variations in local center-of-gravity position as well as in aspect ratio, taper ratio, and sweep angle.

As indicated in reference 1, the modified-strip-analysis method can employ either coupled or uncoupled vibration modes, but the computing program as presently formulated requires uncoupled modes. Therefore, in order to provide a common basis for comparing the two theories, uncoupled modes were used in kernel-function calculations as well as in modified-strip-analysis calculations for all seven wings. In addition, since measured natural (coupled) modes were available for four of the wings, those modes were also employed in some kernel-function calculations for comparison purposes. The natural modes for two of the latter wings involve a high degree of bending-torsion coupling as well as some camber and hence are not closely approximated by uncoupled modes. Examination of the coupled-mode and uncoupled-mode kernel-function calculations should give some indication of whether uncoupled-mode flutter analyses of this type might be expected to yield accurate results for such wings.

SYMBOLS

a_c streamwise distance from leading edge to local aerodynamic center (for steady flow), fraction of streamwise chord (called ac in refs. 1, 2, and 12)

$a_{c,n}$ distance from midchord to local aerodynamic center (for steady flow) measured perpendicular to elastic axis, positive rearward, fraction of local semichord perpendicular to elastic axis (called ac_n in refs. 1, 2, and 12)

b_s streamwise semichord measured at wing root

$c_{l_{\alpha,n}}$ local lift-curve slope for a section perpendicular to elastic axis in steady flow

k reduced frequency at flutter, $b_s\omega/V$

M Mach number

$\overline{m}$ total mass of exposed wing panel

V flutter speed

V_R calculated reference flutter speed obtained from the modified-strip-analysis method by using aerodynamic parameters for two-dimensional incompressible flow

v volume of a conical frustum having streamwise root chord as lower base diameter, streamwise tip chord as upper base diameter, and panel span as height

x streamwise coordinate measured from wing leading edge, positive rearward, fraction of local chord

y' spanwise coordinate measured from plane of symmetry, fraction of semispan

y spanwise coordinate measured from wing panel root, fraction of panel span

z_n normalized local translational displacement of wing in nth natural (coupled) vibration mode

η coordinate measured from wing panel root along elastic axis, fraction of elastic axis length

$\overline{\mu}$ mass ratio, $\overline{m}/\rho v$

ρ air density

ω circular frequency of vibration at flutter

ω_α circular frequency of first uncoupled torsional vibration mode

$\omega_{h,i}$ circular frequency of ith uncoupled bending vibration mode

ω_n circular frequency of nth natural (coupled) vibration mode

WINGS

Wing Designation

For convenience the wing-designation system employed in references 1 and 12 is retained in the present report. In the three-digit system used for the tapered wings, the first digit is the aspect ratio of the full wing to the nearest integer. The second and third digits give the quarter-chord sweep angle to the nearest degree. The letter F or R is appended to the planform designation in order to indicate a wing which has been ballasted to shift its local centers of gravity forward or rearward, respectively. For the untapered wings the same designation system is used, except that a fourth digit 1 is appended to distinguish the taper ratio.

Wing Description

Tapered wings.- All five of the tapered wings treated in this report had aspect ratio 4.0, taper ratio 0.6, and NACA 65A004 airfoils streamwise. All were of essentially homogeneous construction except where segmented ballast weights were imbedded in the wing in order to alter the center-of-gravity position. (See fig. 1(a).) For flutter testing (refs. 9 and 10) these wings were cantilever mounted in the midwing position on a cylindrical sting fuselage with diameter equal to 21.9 percent of the span.

The three 45° swept wings are wings 445, 445F, and 445R of references 1 and 12. Some experimental flutter data as well as the mass and stiffness properties for these wings are given in reference 9.

The two unswept wings are wings 400 and 400R of references 1 and 12. The experimental flutter data and mass and stiffness properties for wing 400 are given in reference 10, and those for wing 400R are given in reference 1.

Untapered wings.- The two untapered wings of this investigation were of solid aluminum construction and had 2.05-percent-thick symmetrical hexagonal airfoil sections perpendicular to the leading edge. One wing was swept back 15° and had an aspect ratio of 5.34 and hence is designated as wing 5151; the other was swept back 30° and had an aspect ratio of 4.16 and hence is called wing 4301 herein. (See fig. 1(b).) These wings were flutter tested (ref. 11) as cantilever-mounted semispan models with no simulated fuselage. The flutter-test data and model properties for these wings are given in reference 11. These two wings were also employed in the flutter analyses of reference 4, in which they were referred to as 15° wing model D and 30° wing model D.

Mode Shapes and Frequencies

Coupled modes.- Natural (coupled) vibration modes were available for the present analyses only for wings 445F, 445R, 5151, and 4301. For wings 445F and 445R, the first three coupled mode shapes (figs. 2 and 3) were measured by a photographic method similar to that described in reference 13. In figures 2 and 3, the symbols show the resulting measured deflections, whereas the curves indicate the least-squares-fitted sixth-degree polynomials which were used to represent the modal deflections in the flutter calculations. It may be noted that points of zero deflection exhibited by the data in figures 2 and 3 agreed very well with node-line locations shown by salt crystals sprinkled on the oscillating wing. Little bending-torsion coupling appears in the first three natural modes of wings 445F and 445R, although some camber occurs along streamwise sections.[2] (See figs. 2 and 3.)

The first three natural mode shapes for wings 5151 and 4301 were measured by a "bouncing-sand" technique and were presented in reference 14. These mode shapes and the corresponding node lines (fig. 1(b) herein) indicate that the second and third natural modes involve a high degree of bending-torsion coupling and some streamwise camber, particularly for wing 4301.

A summary of the measured frequencies for the first three coupled vibration modes of wings 445F, 445R, 5151, and 4301 is given in table I.

Uncoupled modes.- For all flutter calculations employing three uncoupled vibration modes, the mode shapes were assumed to be those associated with the first torsion and first and second bending modes of a uniform cantilever beam. For use in the uncoupled-mode analyses, these mode shapes are correct for the two untapered wings (5151 and 4301) but are, of course, only approximate for the five tapered wings. This mode-shape approximation, however, should have an insignificant effect on the calculated flutter-speed ratios. This expectation is supported by flutter calculations employing both uniform-beam mode shapes and calculated mode shapes for the highly tapered swept-wing planform of reference 3; the results (fig. 26 of ref. 3) showed that use of the uniform-beam mode shapes even for that highly tapered wing raised subsonic flutter-speed ratios only about 2 percent.

For wing 445R, in addition to the three-uniform-beam-mode representation previously described, the first four uncoupled mode shapes (first three bending and first torsion) were calculated by an iteration procedure for use in one set of kernel-function calculations.

For the five tapered wings, the uncoupled-mode frequencies were obtained from the measured natural-mode values since the natural modes involved little bending-torsion coupling. By following the procedure of references 9 and 10,

---

[2]It should be remembered that the use of uncoupled vibration modes to represent the deformations of swept wings also leads to some camber of streamwise sections. For uncoupled modes, wing sections normal to the elastic axis are assumed to oscillate without distortion. Therefore, if these sections do not lie in the free-stream direction, some camber deformation of streamwise sections appears.

measured frequencies for coupled bending modes were used directly as uncoupled bending-mode frequencies. Measured coupled torsion-mode frequencies were "uncoupled" by means of the relation used in references 9 and 10. For wing 445R, the frequency for the iterated third bending mode was extrapolated from the measured second-mode frequency by multiplying by the calculated ratio of third-mode frequency to second-mode frequency.

For the two untapered wings, the uncoupled-mode frequencies were obtained from the simple formulas for a uniform cantilever beam as described in reference 4. The uncoupled mode frequencies for all seven wings are summarized in table I. Note that two sets of uncoupled-mode frequencies are given for wings 445F and 445R. The first set of values for each of these wings was used in the flutter analyses of references 1, 2, and 12 and is considered to be representative for the series of models employed in the experimental flutter investigation of reference 9. The second set of values corresponds to measured coupled-mode frequencies (table I) for the particular models of the same series on which the coupled (natural) mode shapes were measured. (See figs. 2 and 3.)

FLUTTER CALCULATIONS

Modified Strip Analysis

All flutter calculations made by the modified strip method of references 1 and 2 for all seven wings employed three uncoupled vibration modes as previously discussed. The uncoupled-mode frequencies, as well as the other required mass and stiffness parameters, were obtained from the measured wing properties given in references 1 and 9 to 11. All flutter calculations for each of the seven wings were made for a single representative value of flow density with the exception of individual flutter points at $M = 0.60$ for wings 445F and 445R. Reference 12 has shown that calculated subsonic flutter-speed ratios generally are relatively insensitive to density (or mass-ratio) changes. Flutter-frequency ratios, however, are more dependent on the flow density.

Tapered swept wings.- All modified-strip-analysis flutter results shown herein for the three tapered swept wings are reproduced from reference 2 with the exception of individual flutter points at $M = 0.60$ for wings 445F and 445R. The calculations for these three wings at the lower subsonic Mach numbers employed values of steady-flow section lift-curve slope calculated by the lifting-line method of reference 15. The local aerodynamic centers are indicated by this method to be at the quarter chord of streamwise wing sections ($a_c = 1/4$), whereas subsonic steady-flow lifting-surface theory typically indicates aerodynamic centers to be ahead of the quarter chord near the wing tip. (See ref. 3, for example.) However, use of the lifting-line theory in the flutter calculations for these wings is not expected to introduce appreciable errors in the resulting speeds because reference 12 has shown that subsonic flutter speeds calculated for these three wings by the modified strip method are not very sensitive to changes in the local aerodynamic centers. In addition, modified strip analyses for the 45° swept wings of reference 3 showed subsonic flutter speeds obtained by use of lifting-surface aerodynamic parameters to be only

about 6 percent lower than values obtained from lifting-line parameters. The corresponding changes in flutter frequencies were negligible.

For high subsonic, transonic, and low supersonic Mach numbers, steady-flow aerodynamic parameters obtained from wind-tunnel measurements were employed in the flutter calculations. These values were previously used in the flutter calculations of reference 2 and are shown in figures 1 and 2 of that report. Finally, for completeness, supersonic flutter results (ref. 1) employing the linearized lifting-surface theories of references 16 and 17 are also included.

Tapered unswept wings.- All modified-strip-analysis flutter results for the two unswept wings are reproduced from reference 2 with the exception of those from subsonic calculations employing steady-flow aerodynamic parameters obtained from subsonic lifting-surface theory. The calculations of reference 2 used aerodynamic parameters obtained from the subsonic lifting-line method of reference 15 and from the supersonic lifting-surface methods of references 16 and 17. Some flutter calculations from reference 2 in the range $0.6 \leqq M \leqq 0.8$ and at $M = 1.41$ employed values of aerodynamic parameters obtained from wind-tunnel and flight measurements. (See figs. 4 and 6 of ref. 2.) Additional subsonic flutter calculations for the unswept wings have been made with aerodynamic parameters (fig. 4) obtained from subsonic steady-flow lifting-surface theory because reference 12 had shown that calculated flutter speeds for wing 400 could be rather sensitive to changes in local aerodynamic centers. The theory employed is essentially that of reference 18 which also represents the limiting case for the subsonic kernel function as the frequency of oscillation goes to zero.

Untapered swept wings.- All modified-strip-analysis flutter results for the two untapered swept wings (wings 5151 and 4301) are reproduced from reference 4. Calculations for both wings employed steady-flow aerodynamic parameters computed by the lifting-line method of reference 15. In addition, for wing 5151 flutter calculations were made with distributions of aerodynamic parameters obtained from subsonic lifting-surface theory, essentially that of reference 18. All of these aerodynamic parameters are shown in figures 2 and 3 of reference 4.

Subsonic Kernel Function

All subsonic kernel-function flutter calculations were based on the method described in references 7 and 8, and all employed the same values of flow density as were used in the corresponding modified-strip-analysis calculations, with the exception of some calculations for wing 445F in which density was varied. In order to calculate the pressure distribution on an oscillating wing from the equations which relate pressure and downwash, the method of reference 8 treats the lifting pressure as being composed of a linear combination of n assumed pressure modes. The forms of the pressure modes are chosen so that the boundary conditions at the leading edge, trailing edge, and tip are satisfied. The n arbitrary coefficients in the linear combination of pressure modes are evaluated by requiring the pressure-induced downwash to equal that resulting from the wing deflection at n discrete control points on the wing surface.

Tapered swept wings.- In all calculations for the three tapered swept wings, the wing root was taken as a reflection plane. Flutter calculations for all three wings were made with uniform-beam mode shapes (first torsion and first and second bending) as used also in the modified-strip-analysis calculations. In addition, kernel-function calculations were made for wings 445F and 445R with the first three measured coupled mode shapes and frequencies and for wing 445R with the first four uncoupled modes (first three bending and first torsion) calculated by an iteration procedure employing measured mass and stiffness properties.

Most of the kernel-function calculations for these three wings employed nine downwash control (collocation) points which were located at 25, 50, and 75 percent of local streamwise chord from the leading edge and at 30, 60, and 90 percent of the panel span from the root. Some additional calculations for wings 445F and 445R, however, used 16 control points which were located at 20, 40, 60, and 80 percent of local streamwise chord and at 20, 40, 60, and 80 percent of the panel span. (See table II.)

Two sets of calculations for wing 445F included variations in flow density. In calculations with three uncoupled vibration modes and nine control points, density was varied systematically over a wide range. Also, some calculations with 3 coupled modes and 16 control points were made for the specific combinations of Mach number and density at flutter given in table III.

Tapered unswept wings.- In most of the calculations for the two unswept wings, nine downwash control points were taken at 30, 60, and 90 percent of the panel span and at 25, 50, and 75 percent of the local chord with the wing root taken as a reflection plane as for the swept wings. However, an additional calculation was made for wing 400 at $M = 0$ with the control points moved inboard to 20, 50, and 80 percent of the panel span in order to gain some indication of the sensitivity of the resulting flutter speed to control point position. Three uniform-beam vibration modes were employed in all calculations.

In order to indicate the validity of assuming the wing root to be a reflection plane, two additional calculations were made for wing 400 at $M = 0$ and $M = 0.75$. In these additional calculations the reflection plane was taken through the model plane of symmetry which coincided with the center line of the fuselage (fig. 1(a)). The fuselage was not simulated, but the modal deflections were assumed to be composed of uniform-beam modes outboard of the wing root with zero deflection over the inboard portion intercepted by the fuselage.

Untapered swept wings.- The kernel-function calculations for wings 5151 and 4301 were made with three measured coupled vibration modes and with three uncoupled modes. Nine downwash control points were used in each calculation; these points were located at 30, 60, and 90 percent of the panel span and at 25, 50, and 75 percent of the local streamwise chord. (See table II.)

FLUTTER EXPERIMENTS

As indicated previously, experimental flutter data for the seven wings investigated were obtained from references 1 and 9 to 11. However, to provide data at lower Mach numbers for more extensive comparisons with the present calculations, additional flutter experiments have been conducted with wings 445F and 445R. The models used were two that remained from the investigation of reference 9. The model descriptions, test facility, equipment, and technique were the same as in reference 9. For wing 445F the additional flutter points and no-flutter points were measured at Mach numbers from 0.45 to 0.90. For wing 445R two flutter points and a no-flutter point were measured at Mach numbers between 0.48 and 0.60. These new experimental data are summarized in table III.

PRESENTATION OF RESULTS

Flutter speeds calculated by the modified-strip-analysis method and by the subsonic-kernel-function method are compared with measured values for the seven wings in figures 5 to 11. These results are presented in terms of a flutter-speed ratio V/V_R in which the normalizing reference flutter speed V_R for each theoretical or experimental point was calculated by the modified strip method with the density associated with the numerator V and with aerodynamic parameters for two-dimensional incompressible flow $\left(c_{l_{\alpha,n}} = 2\pi \text{ and } a_{c,n} = -1/2\right)$. For flutter speeds V calculated with uncoupled vibration modes, the same mode shapes and frequencies were used in the corresponding V_R calculations. For flutter speeds calculated with coupled modes, the corresponding uncoupled modes were used to calculate V_R. (See table I.) Values of V_R for the experimental points were calculated with three uncoupled modes.

Calculated and measured flutter frequencies for all seven wings are nondimensionalized with respect to the first uncoupled torsion-mode frequency and are shown in figures 12 to 18. Values of reduced frequency at flutter for the three tapered swept wings are given in figures 19 to 21.

The effects of variations in flow density on the calculated flutter-speed ratio and flutter-frequency ratio are shown for wing 445F in figures 22 and 23, respectively.

DISCUSSION OF RESULTS

Tapered Swept Wings

Modified strip analysis.- As shown in reference 2 and in figures 5 to 7 herein, flutter-speed ratios calculated by the modified strip analysis are in

good agreement with the experimental data at all Mach numbers. Further, agreement with the newly measured flutter points at the lower Mach numbers (figs. 6 and 7) is also good.

Calculated flutter frequencies, on the other hand, are in good agreement with measured values at high subsonic and transonic Mach numbers but appear to be somewhat low in the lower subsonic range (figs. 13 and 14). This condition is related at least in part to the use in the flutter calculations of a single representative density rather than the exact experimental value at each point. The measured flutter densities at the lower Mach numbers were considerably higher than the values used in the calculations. Reference 12 showed for these same wings that although subsonic flutter-speed ratios are relatively insensitive to density changes, the corresponding flutter frequencies rise significantly as density increases. To illustrate the magnitude of this density effect, individual flutter points have been calculated for wings 445F and 445R employing measured steady-flow aerodynamic parameters at $M = 0.60$ and using the density and model properties associated with the measured flutter points at the lowest Mach number attained. Figures 6 and 7 show that the increase of density causes a negligible change in the calculated flutter-speed ratio. The calculated frequencies, however, are higher and closer to the experimental values. (See figs. 13 and 14.) Further, figures 26 and 27 of reference 3 indicate that use of calculated mode shapes rather than uniform-beam mode shapes could yield an additional increase in the flutter frequency while causing an insignificant change in the flutter-speed ratio.

Subsonic kernel function.- All kernel-function flutter calculations for the three tapered swept wings yield flutter speeds and frequencies that are higher than those obtained from the modified strip analysis except at the higher subsonic Mach numbers.[3] (See figs. 5 to 7 and 10 to 14.) The maximum differences between flutter-speed ratios calculated by the two methods occur at $M = 0$ and range from 10 percent for wing 445 to as much as 40 percent for wing 445R. In the subsonic range kernel-function flutter speeds for wings 445F and 445R (figs. 6 and 7) are considerably higher than experimental values and indicate a much more pronounced Mach number effect than either the modified-strip-analysis or the flutter experiments. Furthermore, changes in flow density are shown to have only a minor influence on the magnitudes of the differences. Figure 22 shows, however, that as density decreases, the calculated flutter-speed ratio for wing 445F becomes increasingly sensitive to density variation, and differences between kernel-function results and modified-strip-analysis results become greater. In connection with these divergent trends, it may be noted that reference 5 has shown good agreement between flutter speeds and frequencies calculated by the modified strip analysis and corresponding subsonic

[3]In some of the kernel-function calculations of reference 13, two flutter solutions occurred at the higher Mach numbers, one defining an apparently spurious flutter boundary. In reference 13 the flutter speeds associated with these spurious boundaries were in most cases lower than those indicated by the "proper" boundary. For all three tapered swept wings of the present investigation two flutter solutions were encountered over some portion of the Mach number range. In all cases, however, the "second" solutions indicated the higher flutter speeds by a substantial amount. These "second" solutions are therefore not shown in the figures.

experimental values for wings of this same planform at mass ratios from 8 to 260.

As Mach number approaches 1.0, the kernel-function flutter speeds drop steeply to levels well below the experimental values. The latter deviation is perhaps not too surprising inasmuch as the kernel-function procedure was formulated from acoustical theory. Reference 19 shows that as the Mach number approaches 1.0, oscillatory pressure distributions obtained from solutions of the acoustical differential equation ("wave" equation) develop spurious wave-like variations in the chordwise direction. The importance of these oscillations may tend to be mitigated by the surface integrations performed in evaluating the generalized aerodynamic forces, but the results are nevertheless subject to suspicion as M approaches 1.0.

Kernel-function flutter frequencies for wings 445F and 445R appear to be generally in somewhat better agreement with the low Mach number experimental values than are those calculated by the modified strip analysis. Furthermore, use in the flutter calculations of the experimental values of density rather than the single representative value changes the kernel-function flutter frequencies much less than it did for the modified strip analysis. (See also fig. 23.) It should be remembered that effects of density variation are not mitigated in the flutter-frequency ratio as they are in the flutter-speed ratio.

For wings 445F and 445R, use of three measured coupled modes (with nine control points) rather than three uniform-beam modes did not improve the calculated flutter speeds. (See figs. 6 and 7.) The flutter speeds calculated with coupled modes are higher than those calculated with uniform-beam modes at the lower Mach numbers, and the coupled-mode results show greater variation with Mach number. In the coupled-mode calculations, increasing the number of downwash control points from 9 to 16 (the maximum number permissible in the present computing program) caused little change in the resulting flutter speeds at the lower Mach numbers but increased the flutter speeds somewhat at the higher Mach numbers. Thus no improvements in the calculated results were obtained. In comparison with the initial calculations for the three tapered swept wings, which employed three uniform-beam modes and nine control points, improvement in the resulting flutter-speed ratios was obtained only in the low Mach number calculation for wing 445R which included 16 control points and 4 uncoupled modes which were calculated by an iteration process. (See fig. 7.) At all but the highest Mach numbers, however, the latter results are still appreciably above the values indicated by experiment and by the modified strip analysis and still show an excessive decrease of flutter speed with increasing Mach number. In view of the continued poor agreement between these calculations and experiment, no attempt was made in the uncoupled-mode analysis to determine separately the effects of using iterated modes rather than uniform-beam modes, of including the fourth mode, or of increasing the number of control points. For wings 445F and 445R, the changes in the number and type of vibration modes and in the number of control points led to relatively small changes in the calculated flutter frequencies. (See figs. 13 and 14.)

In comparison with the present results, coupled-mode and uncoupled-mode kernel-function flutter speeds and frequencies for the highly tapered 45° swept wing of reference 3 showed relatively little variation with Mach number and were

in satisfactory agreement with experimental data and with results of the modified strip analysis.

In figures 6, 7, 13, 14, 20, and 21, it should be noted that the initial kernel-function calculations for wings 445F and 445R (with three uncoupled modes and nine control points) employed the same representative model properties as those used in most of the calculations by the modified strip method. However, after the low Mach number experimental data became available, the properties of the models used in those investigations were used in all subsequent calculations in an attempt to improve the correlation with those data. The latter models were the ones used in the measurement of the natural (coupled) modes. (See figs. 2 and 3.) The initial representative models and the subsequent specific models differed slightly with regard to mass so that use in the calculations of a single value of flow density for each wing resulted in slight differences in the mass ratio. However, calculations for these two wings by the modified strip method as shown in figures 60 and 61 of reference 12 and in figures 6 and 7 of the present report indicate that these differences in mass ratio (8 percent for wing 445F and 11 percent for wing 445R) should have negligible effects on the calculated flutter-speed ratios. (See also fig. 22.)

In figures 19 to 21, the presentations of reduced frequency contain no normalizing parameter to suppress the effects of differing model properties and flow density which are particularly evident in the experimental data. For example, at a given subsonic Mach number, increasing the flow density characteristically increases the flutter frequency but decreases the flutter speed. Therefore, the calculated curves in figures 19 to 21 should be compared with each other rather than with the experimental points. The experimental values are included for completeness and orientation and should be compared only with the individual calculated points at the same density (square symbols). For constant density at Mach numbers below 0.8, the reduced-frequency values indicated by all calculations for wing 445F are in substantial agreement and show relatively little variation with Mach number. (See fig. 20.) For wing 445R, however, the kernel-function calculations yield k values which decrease as Mach number increases in contrast to the values obtained from the modified strip analysis which slowly increase with M.

The present investigation indicated no clear-cut explanation for the persistent discrepancy between the results of the kernel-function analyses for wings 445F and 445R and the corresponding experimental data and modified-strip-theory calculations. The same model properties were used in both types of analysis. The excitation of vibration modes higher than those included in the present calculations would probably not significantly affect the flutter motion so that their inclusion in the analysis would not be likely to lead to significant improvements in the kernel-function results. The flutter frequencies for these two wings are well below the first-torsion-mode and second-natural-mode frequencies. It may be noted in figure 7 that use of four iterated tapered-beam modes rather than three uniform-beam modes for wing 445R reduces the calculated flutter-speed ratio by a maximum of 8 percent at $M = 0$. At the higher Mach numbers the corresponding change becomes insignificant.

The natural modes for wings 445F and 445R (figs. 2 and 3) do not show evidence of appreciable mass coupling of the type discussed in references 20 and 21

for wings with large concentrated masses. The calculations of references 20 and 21 showed that for satisfactory flutter prediction, more modes were generally required as mass coupling increased. Furthermore, in contrast to the results of reference 20, the flutter speeds obtained from the present kernel-function analyses are unconservative for both forward and rearward ballast locations.

With regard to the aerodynamic representation, it is noted for wings 445F and 445R that flutter speeds calculated with coupled modes by the kernel-function method employing 9 and 16 control points (figs. 6 and 7) differ significantly at the higher Mach numbers. It is possible, therefore, that inclusion of additional control points and pressure modes could produce some further changes in the calculated results. However, there is no reason to believe that convergence of the flutter solution with regard to the number of pressure modes used would be less satisfactory for these wings than for any other wing of more or less conventional configuration.

Tapered Unswept Wings

Modified strip analysis.- Subsonic flutter speeds calculated for the two unswept wings by the modified strip analysis employing steady-flow aerodynamic parameters obtained from lifting-surface theory are lower (by about 7 percent for wing 400 and by about 5 percent for wing 400R) and in better agreement with experiment than those calculated by use of lifting-line aerodynamics. (See figs. 8 and 9.) The reason for this reduction of calculated flutter speed is indicated in figure 4. As stated previously and illustrated in figure 4, the major difference between aerodynamic parameters calculated by lifting-line theory and by lifting-surface theory occurs in the aerodynamic-center locations near the wing tip. In particular, the more forward aerodynamic centers for the lifting-surface theory together with moderate sensitivity of unswept-wing flutter speeds to changes in the aerodynamic centers produce the reductions in flutter speed shown in figures 8 and 9. Figures 15 and 16 again show, however, that these aerodynamic changes have little effect on the flutter frequency.

With regard to the use of a single representative value of density in the calculations for the unswept wings, figures 65 and 66 of reference 12 indicate for wings 400 and 400R virtually no sensitivity of subsonic flutter-speed ratio to changes in density. Figures 76 and 77 of that reference, however, show some variation of flutter frequency with density.

Subsonic kernel function.- Flutter speeds for the two unswept wings (figs. 8 and 9) calculated by the kernel-function method with three uncoupled vibration modes are in good agreement with the results of the modified strip analysis and with the experimental data. Again the largest differences between the two theories appear at $M = 0$, but for the unswept wings these differences are relatively small. As the Mach number approaches 1.0, the kernel-function flutter speeds for wing 400 turn sharply upward in contrast to the corresponding trends for the swept wings.

For wing 400, flutter frequencies calculated by the kernel function are in better agreement with the experimental values than are those obtained by the

modified strip analysis. For wing 400R, however, flutter frequencies calculated by both methods are in satisfactory agreement with experiment.

Figures 8 and 15 show that insignificant changes in both flutter speed and frequency for wing 400 result from the spanwise relocation of the downwash control points previously discussed. These same figures show that making the kernel-function calculations for the full semispan rather than for the exposed wing panel also leads to insignificant changes in the flutter characteristics.

Untapered Swept Wings

Modified strip analysis.- Flutter speeds calculated by the modified strip method for wings 5151 and 4301 are in good agreement with experimental values (figs. 10 and 11 and ref. 4), although the calculated frequencies are somewhat low. The flutter speeds for wing 5151 calculated from lifting-surface aerodynamic parameters are somewhat lower than those obtained with lifting-line aerodynamics. As indicated previously, this result typically appears because the local aerodynamic centers given by lifting-surface theory are generally forward of those indicated by lifting-line theory, especially near the wing tips. (See fig. 2 of ref. 4, for example.)

Subsonic kernel function.- The flutter-speed curves calculated for wing 5151 by coupled-mode and uncoupled-mode kernel-function analyses (fig. 10) closely bracket the experimental flutter point and do not differ significantly from each other except at the lowest Mach numbers. Flutter speeds calculated by the modified strip analysis are in good agreement with values obtained from the coupled-mode kernel-function analysis. At the higher Mach numbers, the two kernel-function flutter-speed curves appear to converge, and both show a decrease in flutter speed with increasing Mach number that is not indicated by the modified strip analysis, at least up to $M = 0.75$. The flutter frequencies calculated by the kernel-function analyses (fig. 17) are in satisfactory agreement with the experimental value.

For wing 4301, the coupled- and uncoupled-mode kernel-function analyses gave flutter speeds that are close together through the Mach number range and in good agreement with experiment and with the modified strip analysis. (See fig. 11.) The flutter frequencies calculated with coupled modes are in good agreement with the experimental point, whereas the values obtained with uncoupled modes are somewhat lower but still in satisfactory agreement with the data point. (See fig. 18.)

These kernel-function results show no large adverse effects on the calculated flutter speeds and frequencies resulting from the use of uncoupled modes in the analyses for these two wings, even though their natural modes were highly coupled. In comparison, the flutter analyses for the highly tapered swept wings of reference 3 also indicated little difference between flutter speeds obtained from coupled-mode and uncoupled-mode calculations by the subsonic kernel-function method, although the coupled modes for those wings contained considerably more camber than the modes for the present wings. The results of both types of kernel-function calculations as well as of modified-strip-theory calculations (with uncoupled modes) were in good agreement with experiment.

CONCLUSIONS

Subsonic flutter characteristics for seven swept and unswept wings have been calculated by the kernel-function method and by a modified strip method. Comparisons of the results with flutter experiments indicate the following conclusions:

1. Flutter speeds calculated by the modified strip method for all seven wings are in good agreement with experimental values.

2. Flutter speeds calculated by the kernel-function method are in good agreement with experiment and with results of the modified strip method for five of the wings.

3. For the two swept wings which had ballast weight distributed along leading or trailing edges, flutter speeds predicted by the kernel-function method were unconservative by an appreciable amount at the lower Mach numbers. At the higher Mach numbers, these calculations showed a rapid drop in flutter speed which was not confirmed by experiment nor by values calculated from the modified strip method. These kernel-function results were not particularly sensitive to variations in flow density and were not significantly improved by changes in the number or type of vibration modes (coupled or uncoupled) nor by increasing the number of downwash control (collocation) points.

4. Coupled-mode and uncoupled-mode kernel-function analyses for two homogeneous untapered swept wings yielded flutter speeds that were close together for each wing and in good agreement with experiment and with results from the modified strip method. Thus, the high degree of bending-torsion coupling which appeared in the natural (coupled) modes for these wings had no appreciable effect on the analytical results.

Langley Research Center,
National Aeronautics and Space Administration,
Langley Station, Hampton, Va., February 13, 1964.

REFERENCES

1. Yates, E. Carson, Jr.: Calculation of Flutter Characteristics for Finite-Span Swept or Unswept Wings at Subsonic and Supersonic Speeds by a Modified Strip Analysis. NACA RM L57L10, 1958.

2. Yates, E. Carson, Jr.: Use of Experimental Steady-Flow Aerodynamic Parameters in the Calculation of Flutter Characteristics for Finite-Span Swept or Unswept Wings at Subsonic, Transonic, and Supersonic Speeds. NASA TM X-183, 1960.

3. Yates, E. Carson, Jr.: Subsonic and Supersonic Flutter Analysis of a Highly Tapered Swept-Wing Planform, Including Effects of Density Variation and Finite Wing Thickness, and Comparison With Experiments. NASA TM X-764, 1963.

4. Yates, E. Carson, Jr., and Bennett, Robert M.: Use of Aerodynamic Parameters From Nonlinear Theory in Modified-Strip-Analysis Flutter Calculations for Finite-Span Wings at Supersonic Speeds. NASA TN D-1824, 1963.

5. Yates, E. Carson, Jr., Land, Norman S., and Foughner, Jerome T., Jr.: Measured and Calculated Subsonic and Transonic Flutter Characteristics of a 45° Sweptback Wing Planform in Air and in Freon-12 in the Langley Transonic Dynamics Tunnel. NASA TN D-1616, 1963.

6. Bennett, Robert M., and Yates, E. Carson, Jr.: A Study of Several Factors Affecting the Flutter Characteristics Calculated for Two Swept Wings by Piston Theory and by Quasi-Steady Second-Order Theory and Comparison With Experiments. NASA TN D-1794, 1963.

7. Watkins, Charles E., Runyan, Harry L., and Woolston, Donald S.: On Kernel Function of the Integral Equation Relating the Lift and Downwash Distributions of Oscillating Finite Wings in Subsonic Flow. NACA Rep. 1234, 1955. (Supersedes NACA TN 3131.)

8. Watkins, Charles E., Woolston, Donald S., and Cunningham, Herbert J.: A Systematic Kernel Function Procedure for Determining Aerodynamic Forces on Oscillating or Steady Finite Wings at Subsonic Speeds. NASA TR R-48, 1959.

9. Jones, George W., Jr., and Unangst, John R.: Investigation to Determine Effects of Center-of-Gravity Location on Transonic Flutter Characteristics of a 45° Sweptback Wing. NACA RM L55K30, 1956.

10. Unangst, John R., and Jones, George W., Jr.: Some Effects of Sweep and Aspect Ratio on the Transonic Flutter Characteristics of a Series of Thin Cantilever Wings Having a Taper Ratio of 0.6. NASA TN D-1594, 1963. (Supersedes NACA RM L55I13a and NACA RM L53G10a.)

11. Tuovila, W. J., and McCarty, John Locke: Experimental Flutter Results for Cantilever-Wing Models at Mach Numbers up to 3.0. NACA RM L55E11, 1955.

12. Yates, E. Carson, Jr.: Some Effects of Variations in Density and Aerodynamic Parameters on the Calculated Flutter Characteristics of Finite-Span Swept and Unswept Wings at Subsonic and Supersonic Speeds. NASA TM X-182, 1960.

13. Walberg, Gerald D.: Subsonic Kernel-Function Flutter Analysis of a Highly Tapered Tail Surface and Comparison With Experimental Results. NASA TN D-379, 1960.

14. Hanson, Perry W., and Tuovila, W. J.: Experimentally Determined Natural Vibration Modes of Some Cantilever-Wing Flutter Models by Using an Acceleration Method. NACA TN 4010, 1957.

15. DeYoung, John, and Harper, Charles W.: Theoretical Symmetric Span Loading at Subsonic Speeds for Wings Having Arbitrary Plan Form. NACA Rep. 921, 1948.

16. Cohen, Doris: Formulas for the Supersonic Loading, Lift, and Drag of Flat Swept-Back Wings With Leading Edges Behind the Mach Lines. NACA Rep. 1050, 1951.

17. Lagerstrom, P. A., and Wall, D.: Formulas in Three-Dimensional Wing Theory. Rep. No. SM 11901, Douglas Aircraft Co., Inc., July 8, 1946.

18. Falkner, V. M.: The Calculation of Aerodynamic Loading on Surfaces of Any Shape. R & M. No. 1910, British A.R.C., Aug. 1943.

19. Landahl, Marten T.: Theoretical Studies of Unsteady Transonic Flow - Part I. Linearization of the Equations of Motion. FFA Rep. 77, Aero. Res. Inst. of Sweden (Stockholm), 1958.

20. Woolston, Donald S., and Runyan, Harry L.: Appraisal of Method of Flutter Analysis Based on Chosen Modes by Comparison With Experiment for Cases of Large Mass Coupling. NACA TN 1902, 1949.

21. Woolston, Donald S., and Runyan, Harry L.: On the Use of Coupled Modal Functions in Flutter Analysis. NACA TN 2375, 1951.

TABLE I.- SUMMARY OF MODAL FREQUENCIES USED IN CALCULATIONS

Wing	Uncoupled modes				Coupled modes		
	$\omega_{h,1}$, $\frac{\text{radians}}{\text{sec}}$	$\omega_{h,2}$, $\frac{\text{radians}}{\text{sec}}$	$\omega_{h,3}$, $\frac{\text{radians}}{\text{sec}}$	ω_{α}, $\frac{\text{radians}}{\text{sec}}$	ω_1, $\frac{\text{radians}}{\text{sec}}$	ω_2, $\frac{\text{radians}}{\text{sec}}$	ω_3, $\frac{\text{radians}}{\text{sec}}$
400	946	4416	----	2463	---	----	----
400R	570	2811	----	1982	---	----	----
445	411	2274	----	2192	---	----	----
445F	385 355	2070 1948	---- ----	1144 1108	--- 355	---- 1382	---- 1948
445R	320 285	1459 1470	---- 3791	2306 2126	--- 285	---- 1470	---- 2218
5151	251	1575	----	1488	226	1319	1520
4301	240	1501	----	1376	220	1319	1696

TABLE II.- INDEX TO FLUTTER CALCULATIONS

Wing	Modified strip analysis[a] - Source of aerodynamic parameters	Kernel-function analysis: Control points: Number	Control points: Locations: x	Control points: Locations: y	Vibration modes: Number	Vibration modes: Type	Figures in which results are shown for - V/V_R	ω/ω_α	k
445	Lifting-surface theory Lifting-line theory Wind-tunnel test	9	0.25, .50, .75	0.30, .60, .90	3	Uncoupled	5	12	19
445F	Lifting-surface theory Lifting-line theory Wind-tunnel test	9 9 16	0.25, .50, .75 .25, .50, .75 .20, .40, .60, .80	0.30, .60, .90 .30, .60, .90 .20, .40, .60, .80	3 3 3	Uncoupled Coupled Coupled	6, 22	13, 23	20
445R	Lifting-surface theory Lifting-line theory Wind-tunnel test	9 9 16 16	0.25, .50, .75 .25, .50, .75 .20, .40, .60, .80 .20, .40, .60, .80	0.30, .60, .90 .30, .60, .90 .20, .40, .60, .80 .20, .40, .60, .80	3 3 3 4	Uncoupled Coupled Coupled Uncoupled	7	14	21
400	Lifting-surface theory Lifting-line theory Wind-tunnel test X-1E flight test	9 9 9	0.25, .50, .75 .25, .50, .75 .25, .50, .75	0.30, .60, .90 .20, .50, .80 .104, .488, .872[b]	3 3 3	Uncoupled Uncoupled Uncoupled	8	15	--
400R	Lifting-surface theory Lifting-line theory Wind-tunnel test X-1E flight test	9	0.25, .50, .75	0.30, .60, .90	3	Uncoupled	9	16	--
5151	Lifting-surface theory Lifting-line theory	9 9	0.25, .50, .75 .25, .50, .75	0.30, .60, .90 .30, .60, .90	3 3	Uncoupled Coupled	10	17	--
4301	Lifting-line theory	9 9	0.25, .50, .75 .25, .50, .75	0.30, .60, .90 .30, .60, .90	3 3	Uncoupled Coupled	11	18	--

[a] All modified-strip-analysis calculations employ three uncoupled vibration modes.

[b] These stations correspond to y = 0.30, 0.60, 0.90.

TABLE III.- SUMMARY OF EXPERIMENTAL DATA

(a) Modal frequencies for models tested

Wing	Panel	ω_1, $\frac{\text{radians}}{\text{sec}}$	ω_2, $\frac{\text{radians}}{\text{sec}}$	ω_3, $\frac{\text{radians}}{\text{sec}}$	ω_α, $\frac{\text{radians}}{\text{sec}}$
445F	Left	363	1414	2205	----
445F	Right	364	1445	2124	1195
445R	Left	320	1470	2381	2317
445R	Right	285	1470	2218	2126

(b) Flutter results

Wing	Wing behavior		M	ρ, $\frac{\text{slug}}{\text{cu ft}}$	V, $\frac{\text{ft}}{\text{sec}}$	ω, $\frac{\text{radians}}{\text{sec}}$	V/V_R	ω/ω_α
	Left	Right						
445F	No flutter	No flutter	0.457	0.01118	473	----	0.962	-----
445F	No flutter	No flutter	.503	.01035	538	----	1.036	-----
445F	No flutter	Start of flutter	.540	.00894	584	942	1.064	0.788
445F	No flutter	Start of flutter	.640	.00576	693	----	1.054	-----
445F	No flutter	No flutter	.644	.00538	688	----	1.017	-----
445F	No flutter	Start of flutter	.694	.00484	745	880	1.054	.736
445F	No flutter	Start of flutter	.733	.00438	777	864	1.057	.723
445F	No flutter	Start of flutter	.790	.00376	827	848	1.057	.710
445F	No flutter	Start of flutter	.825	.00327	867	817	1.049	.684
445F	No flutter	Start of flutter	.863	.00298	898	792	1.046	.662
445R	No flutter	No flutter	.492	.00753	574	----	1.030	-----
445R	Start of flutter		.583	.00755	619	1005	1.069	.434
445R		Start of flutter	.582	.00755	618	994	1.114	.467

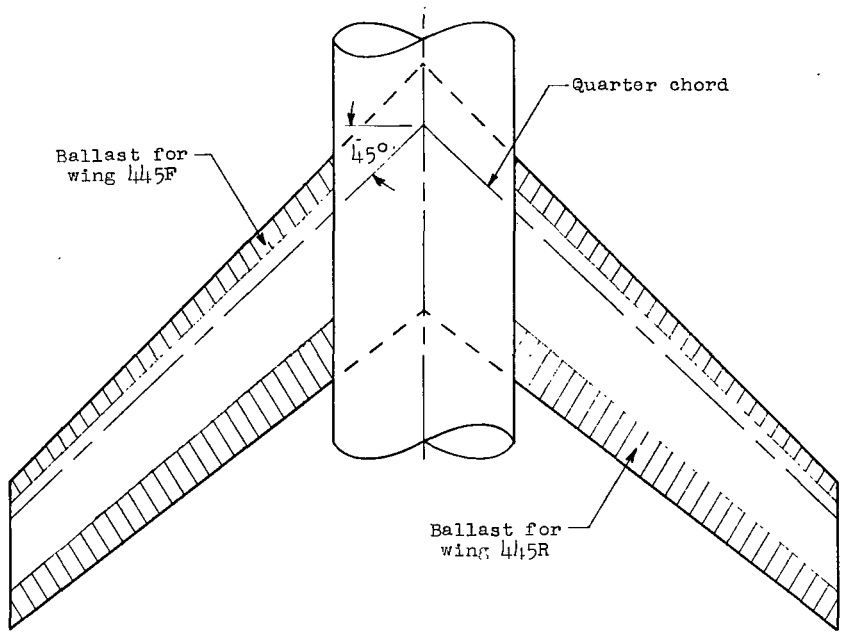

Wings 445, 445F, and 445R

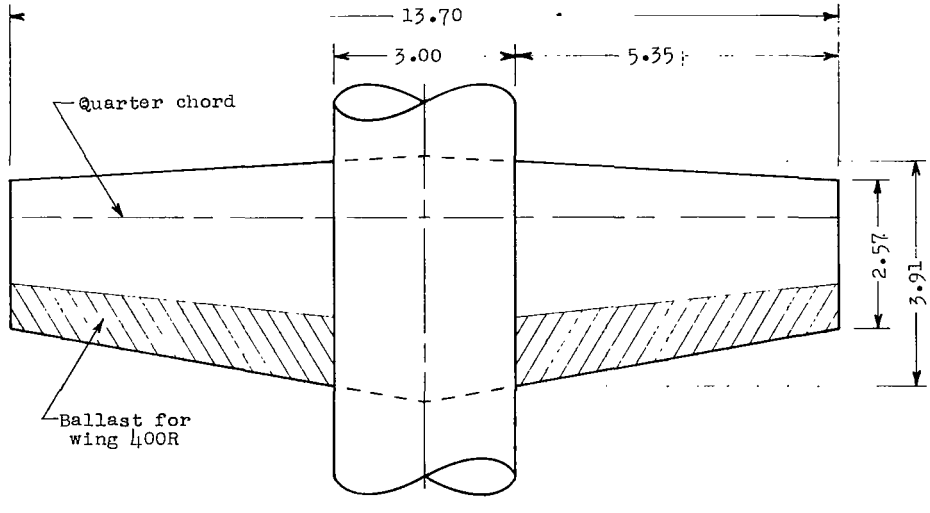

Wings 400 and 400R

(a) Tapered wings. All linear dimensions shown apply to all five wings.

Figure 1.- Wings employed in flutter investigation. All dimensions are in inches unless otherwise specified.

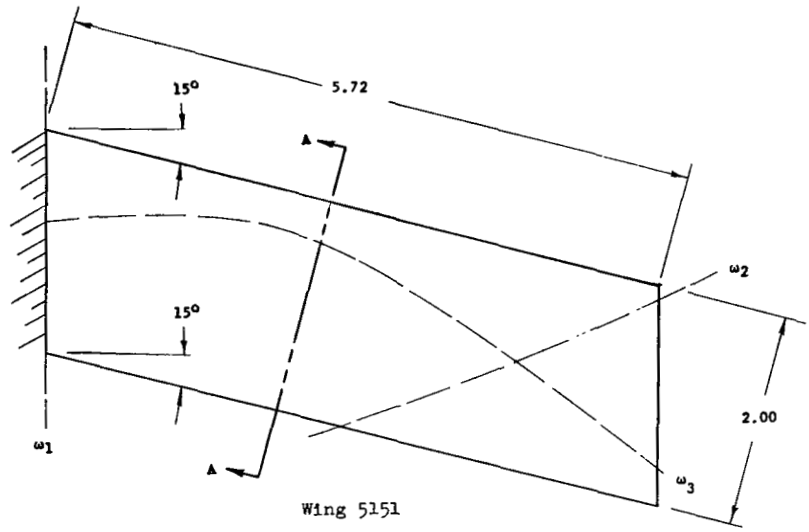

Wing 5151

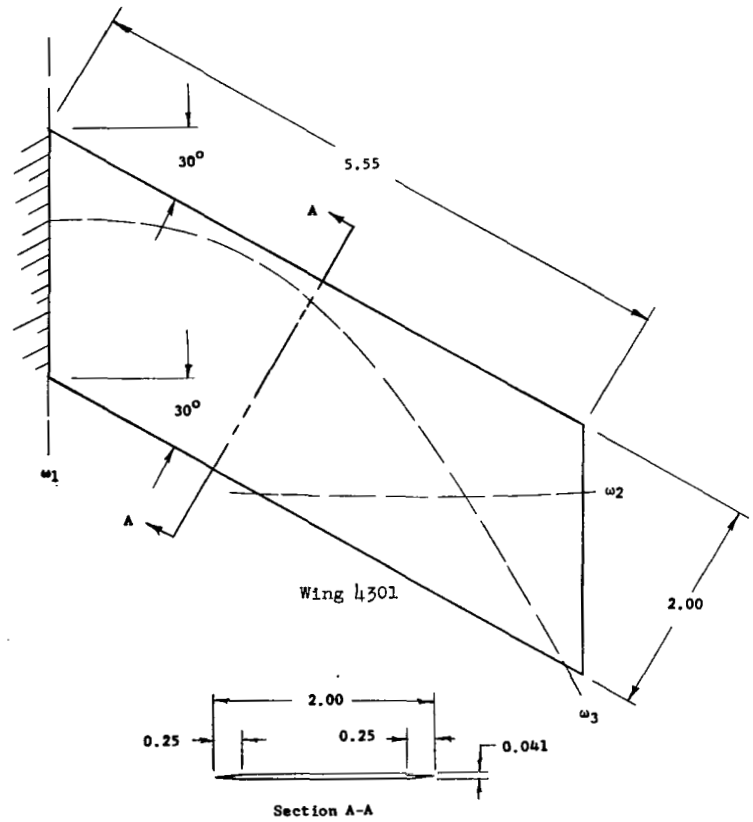

Wing 4301

Section A-A

(b) Untapered wings. Dashed lines indicate measured node lines.

Figure 1.- Concluded.

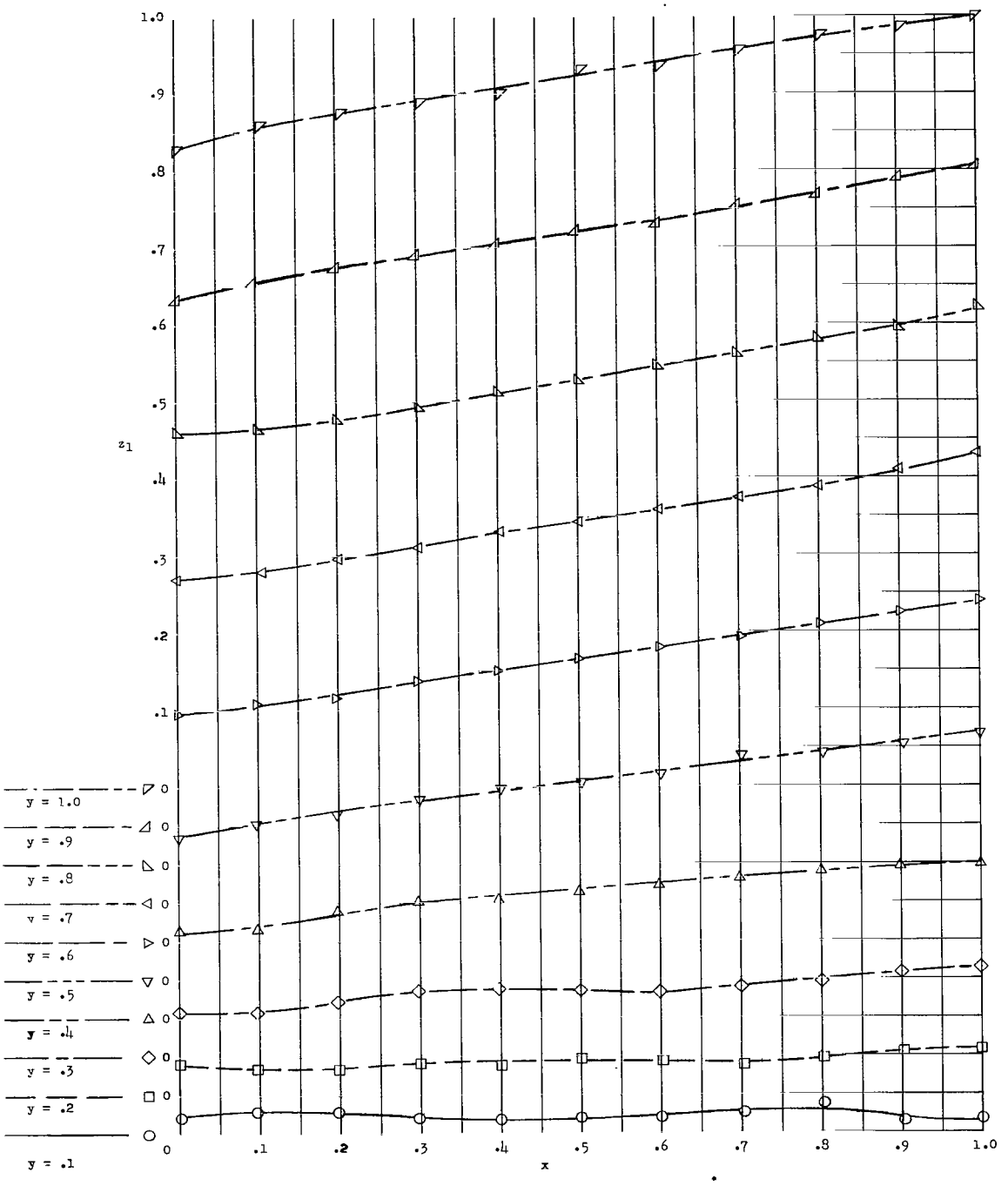

(a) First mode; ω_1 = 355 radians/sec.

Figure 2.- Coupled vibration modes for wing 445F. Symbols indicate measured deflections; curves indicate least-squares-fitted sixth-degree polynomials.

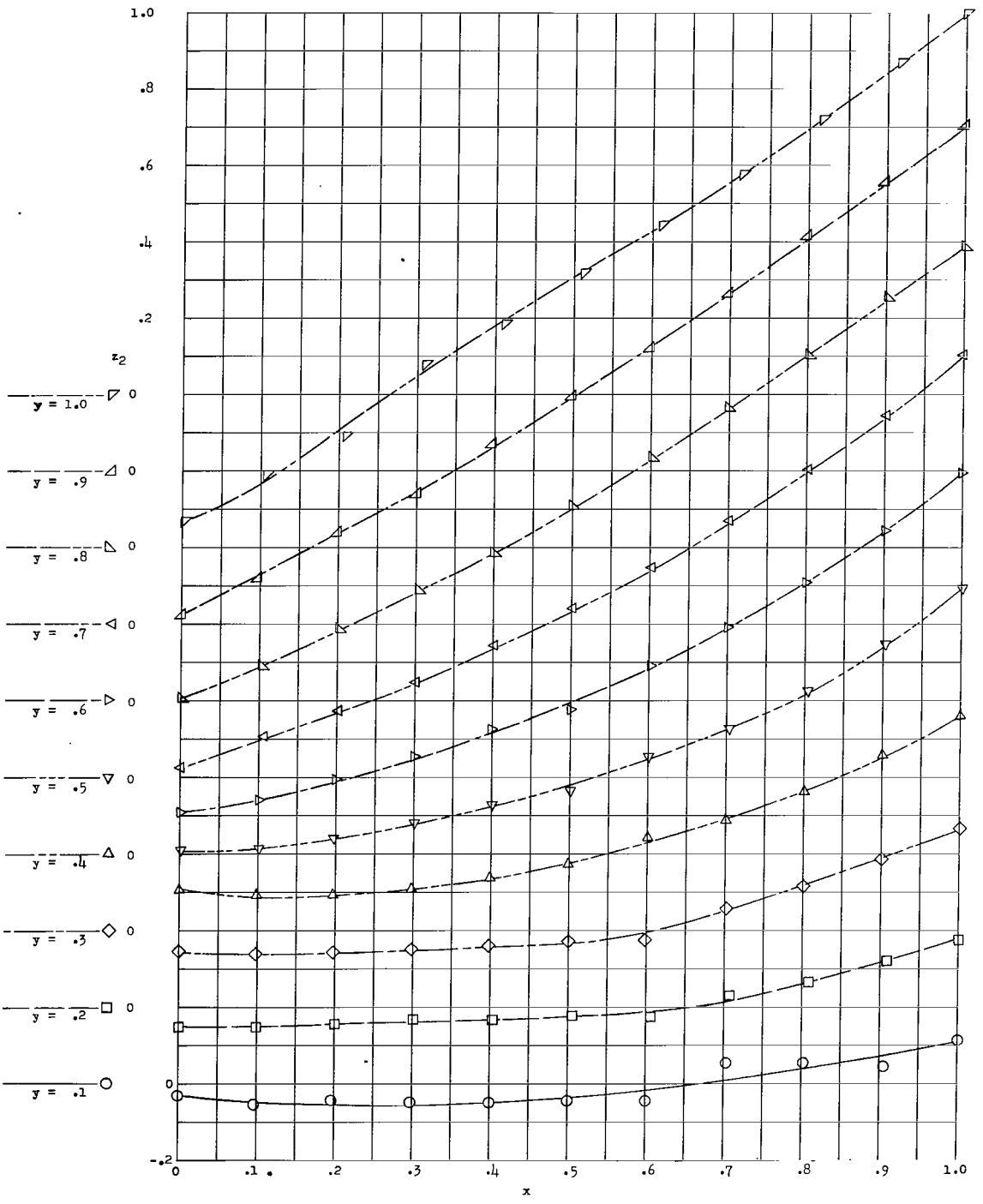

(b) Second mode; ω_2 = 1382 radians/sec.

Figure 2.- Continued.

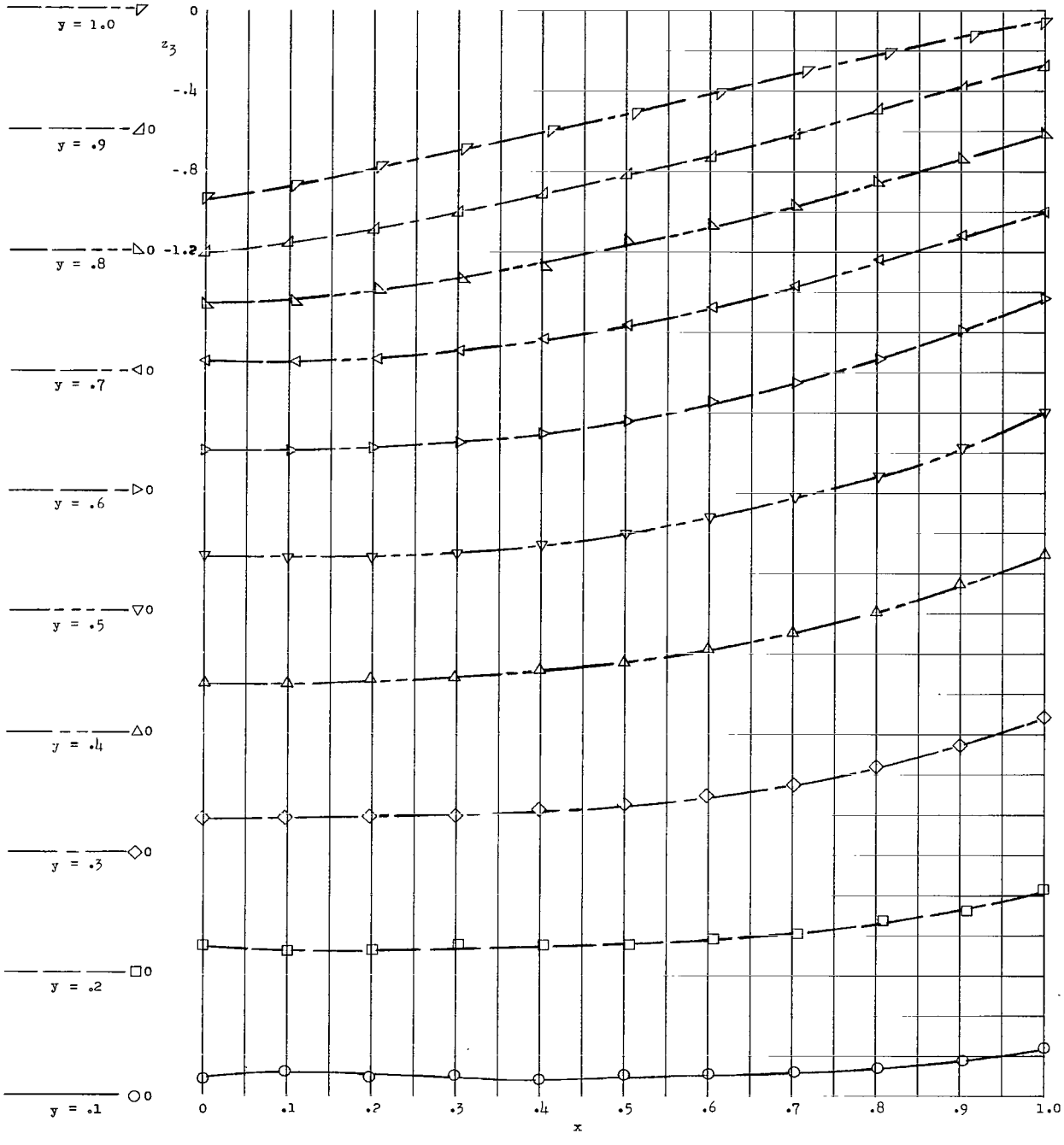

(c) Third mode; ω_3 = 1948 radians/sec.

Figure 2.- Concluded.

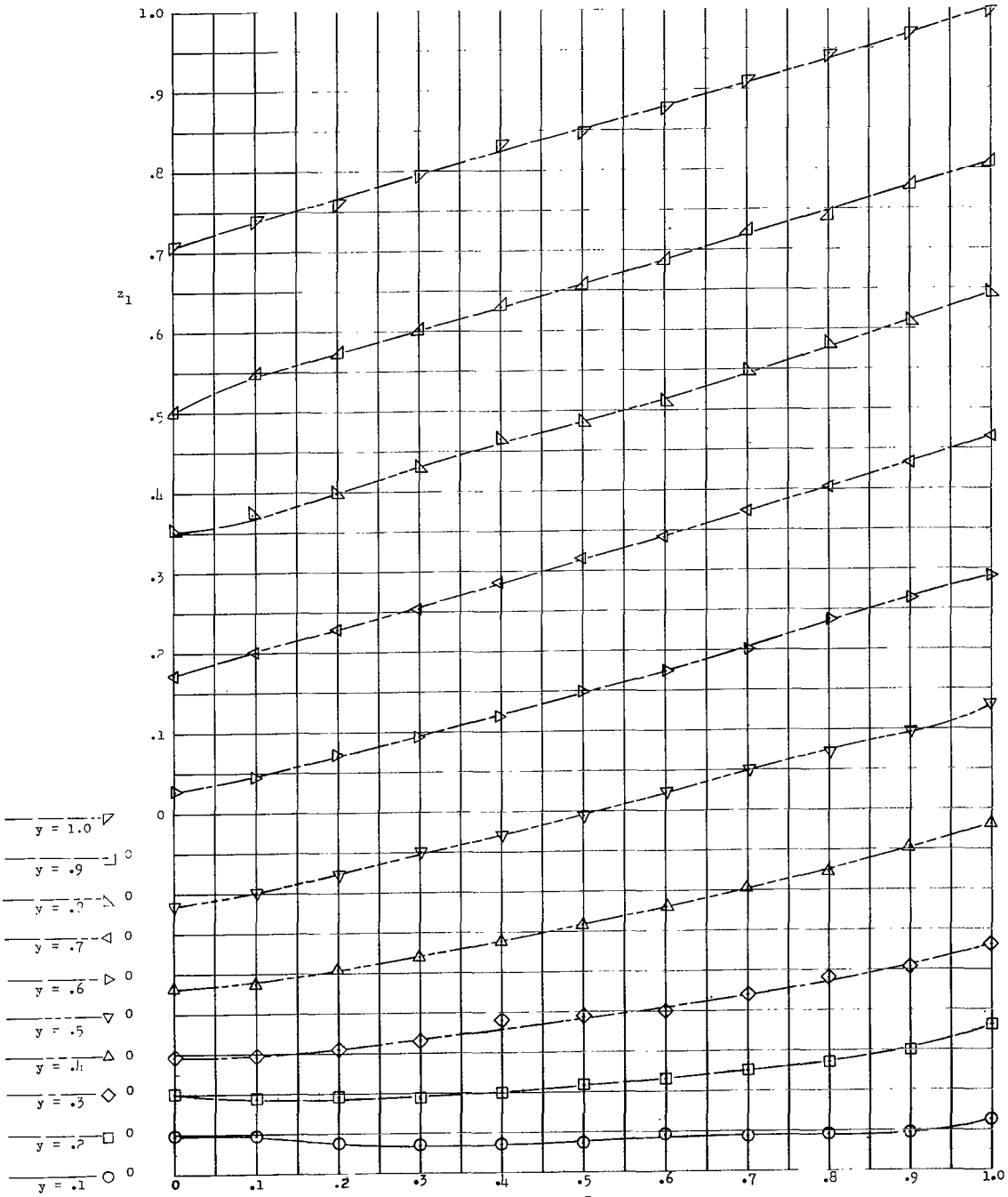

(a) First mode; ω_1 = 285 radians/sec.

Figure 3.- Coupled vibration modes for wing 445R. Symbols indicate measured deflections; curves indicate least-squares-fitted sixth-degree polynomials.

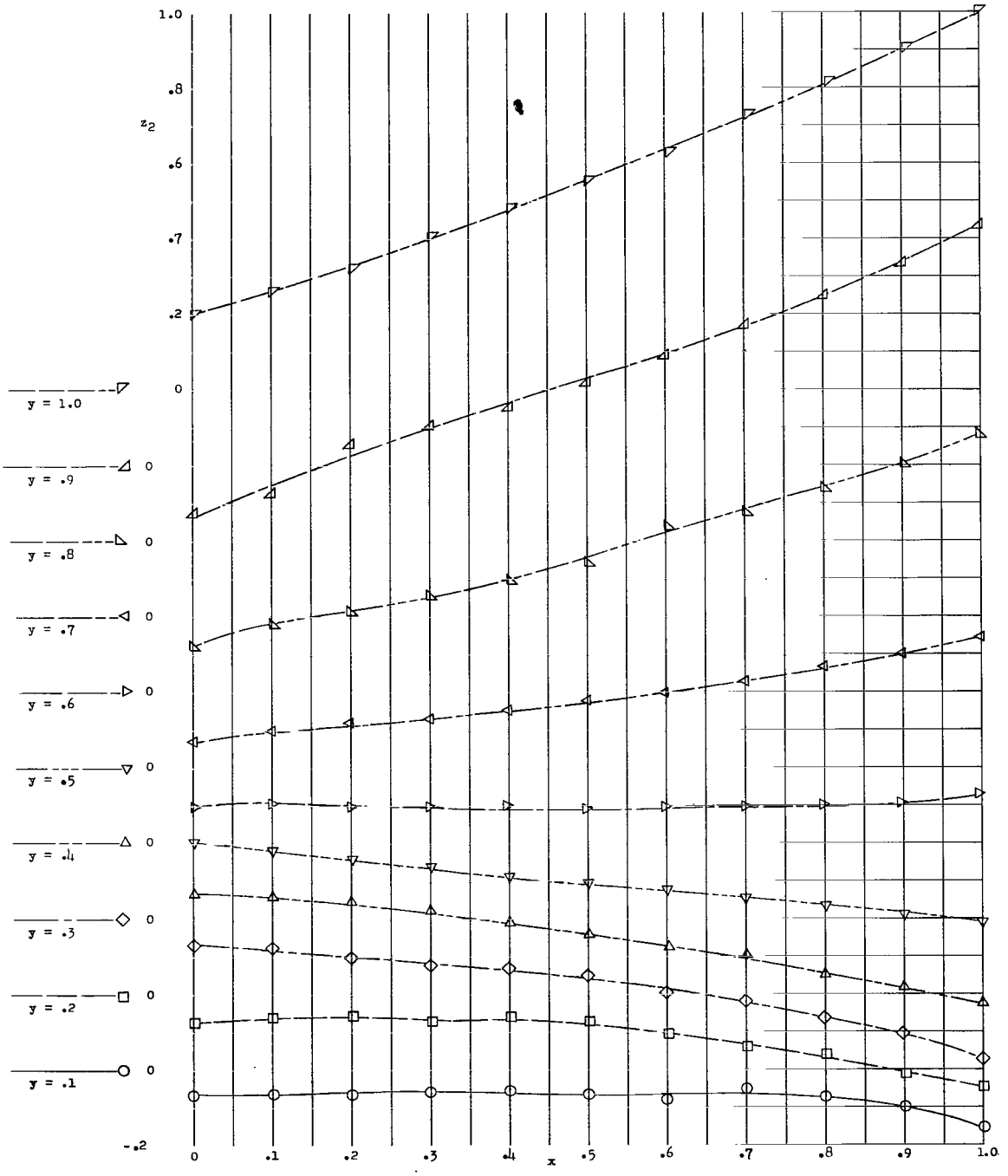

(b) Second mode; ω_2 = 1470 radians/sec.

Figure 3.- Continued.

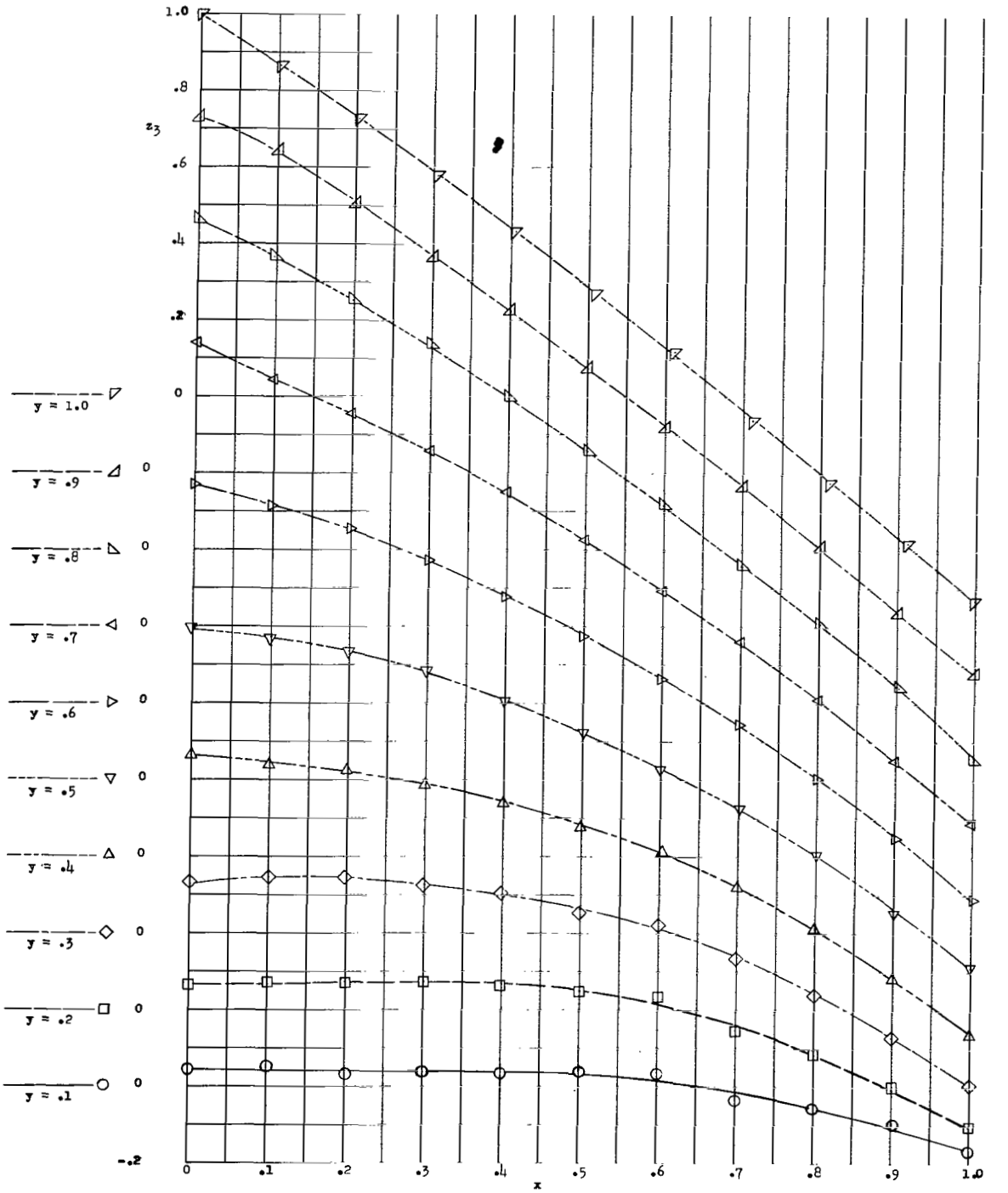

(c) Third mode; ω_3 = 2218 radians/sec.

Figure 3.- Concluded.

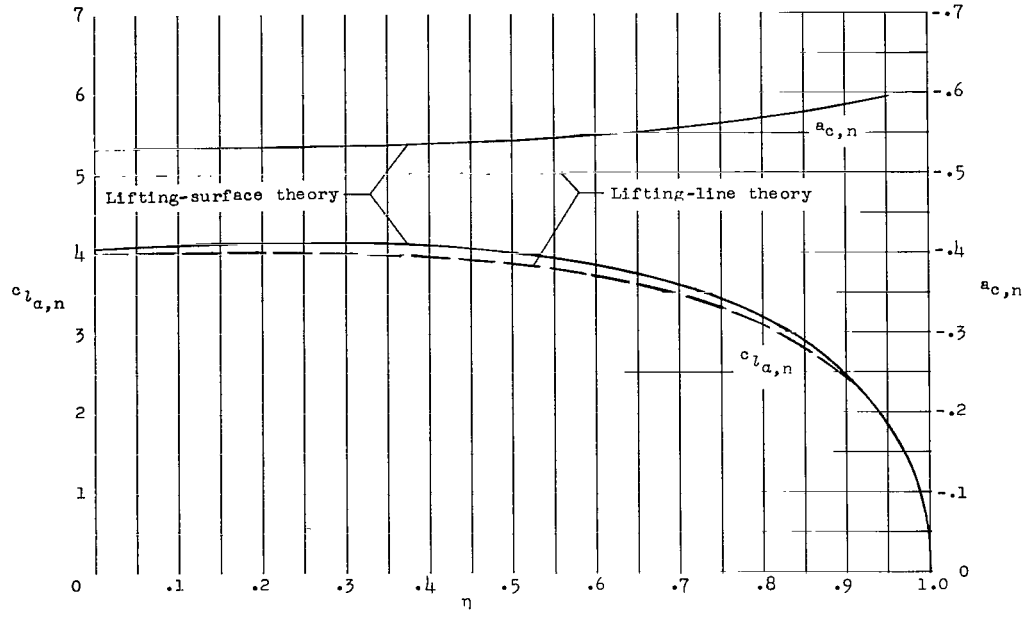

(a) M = 0.

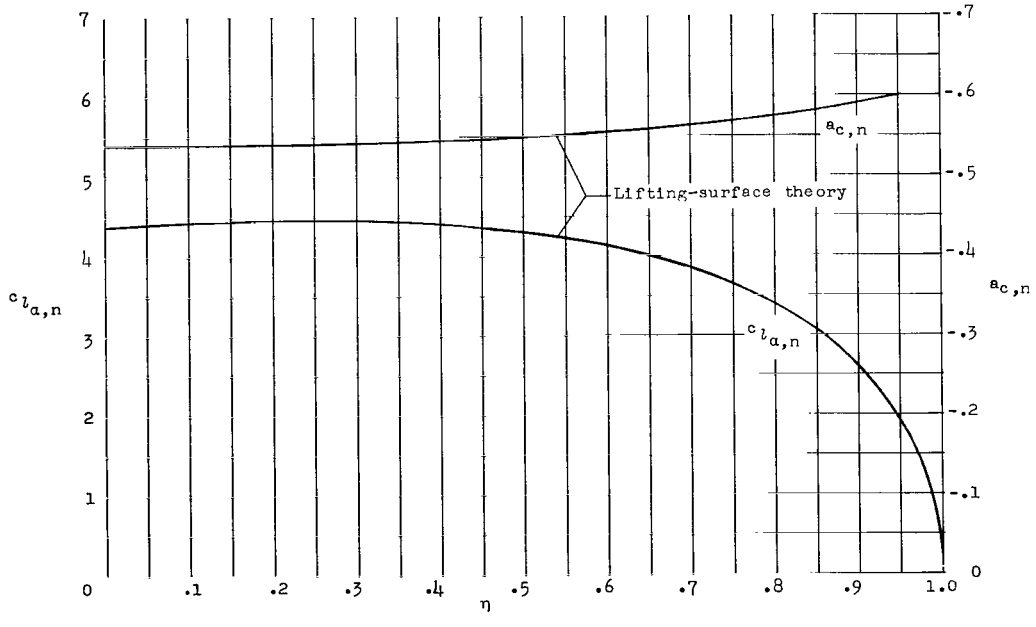

(b) M = 0.50.

Figure 4.- Spanwise distributions of steady-flow aerodynamic parameters for wings 400 and 400R.

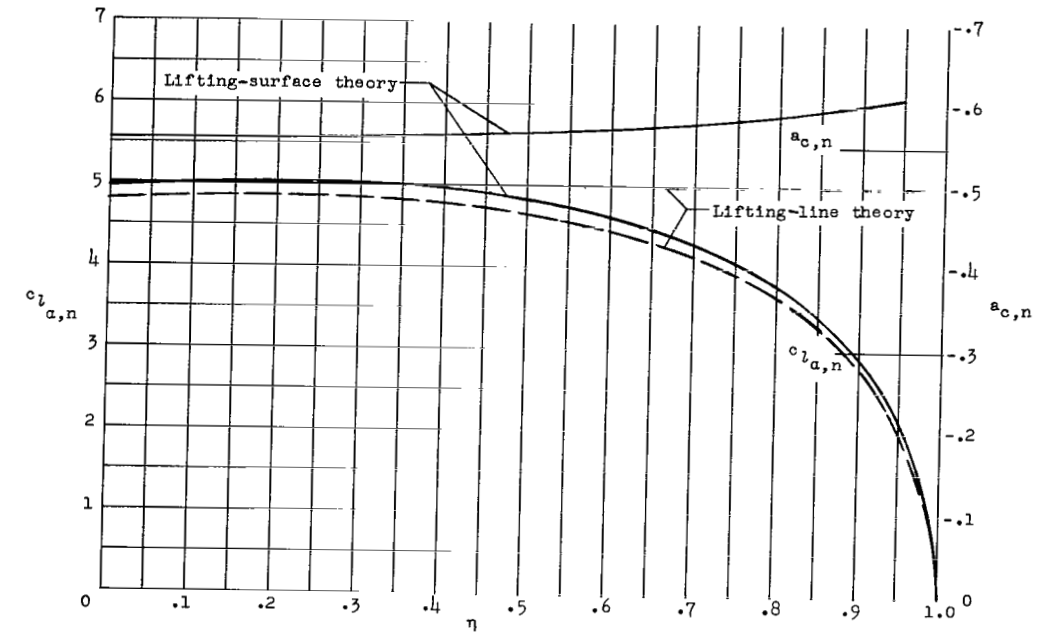

(c) M = 0.75.

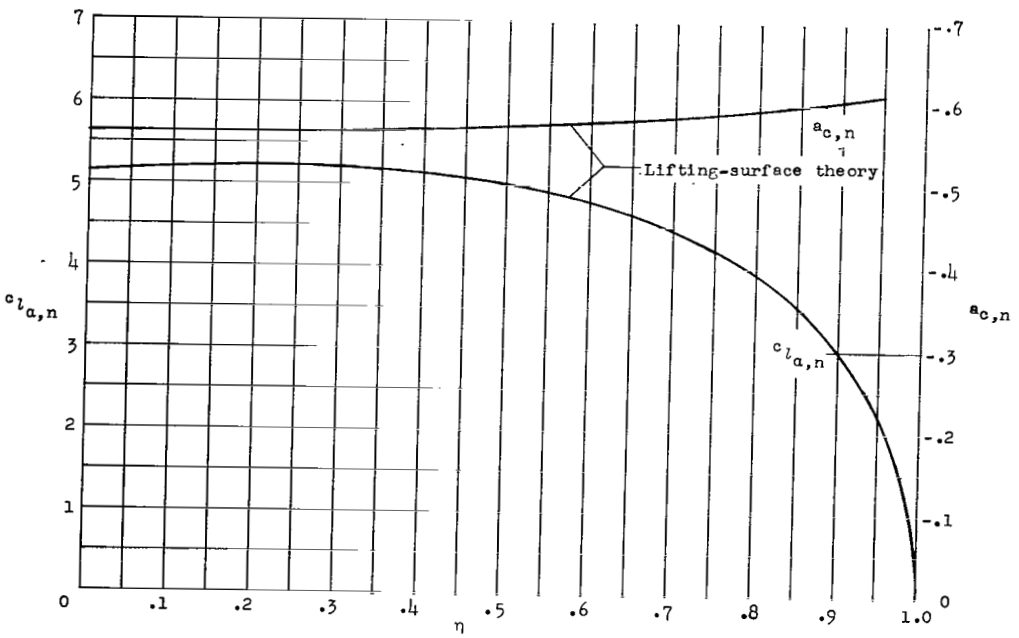

(d) M = 0.80.

Figure 4.- Concluded.

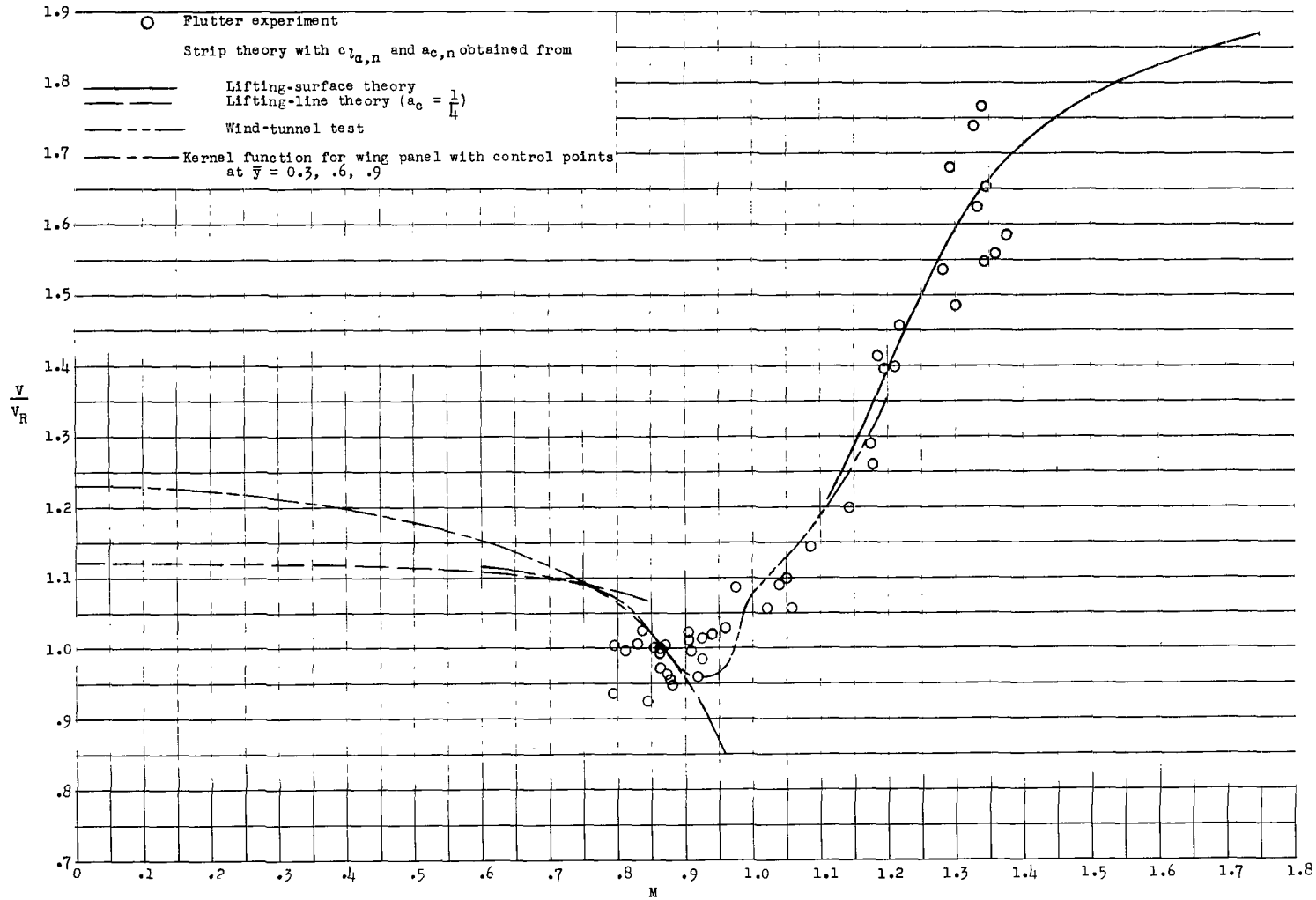

Figure 5.- Variation of flutter-speed ratio with Mach number for wing 445. For calculated points ρ = 0.003800 slug/cu ft and V_R = 735.0 ft/sec. Three uncoupled vibration modes were used in all calculations.

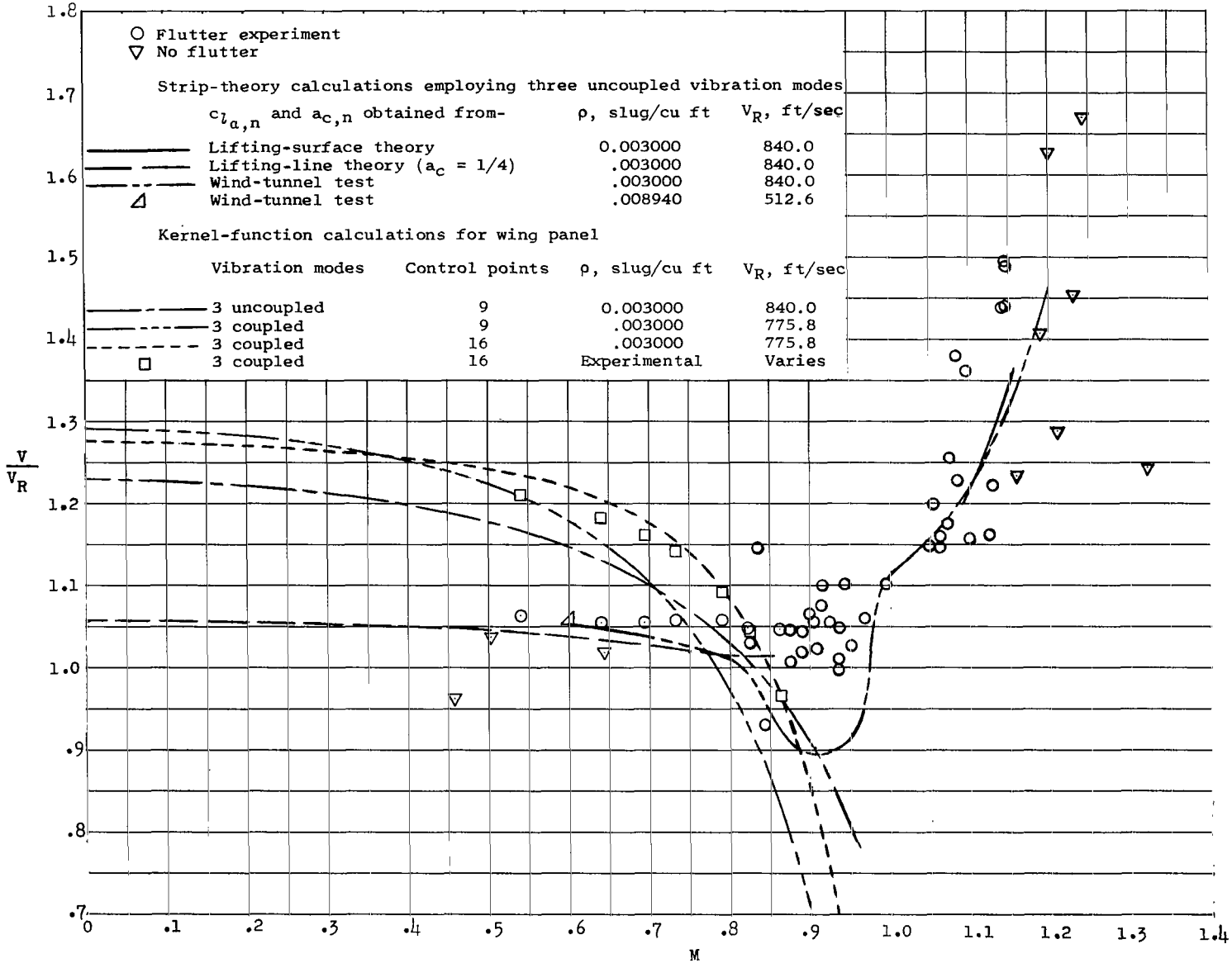

Figure 6.- Variation of flutter-speed ratio with Mach number for wing 445F.

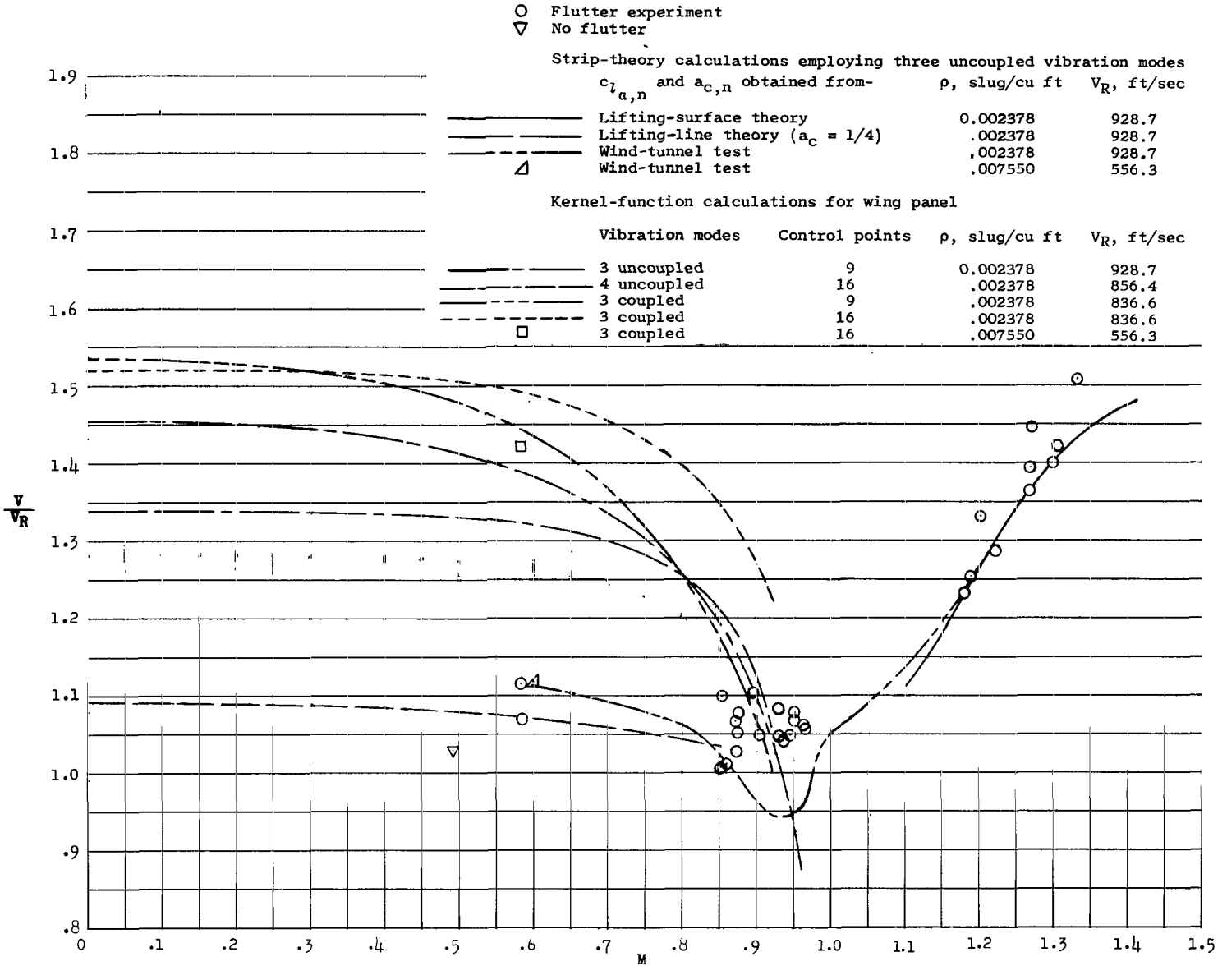

Figure 7.- Variation of flutter-speed ratio with Mach number for wing 445R.

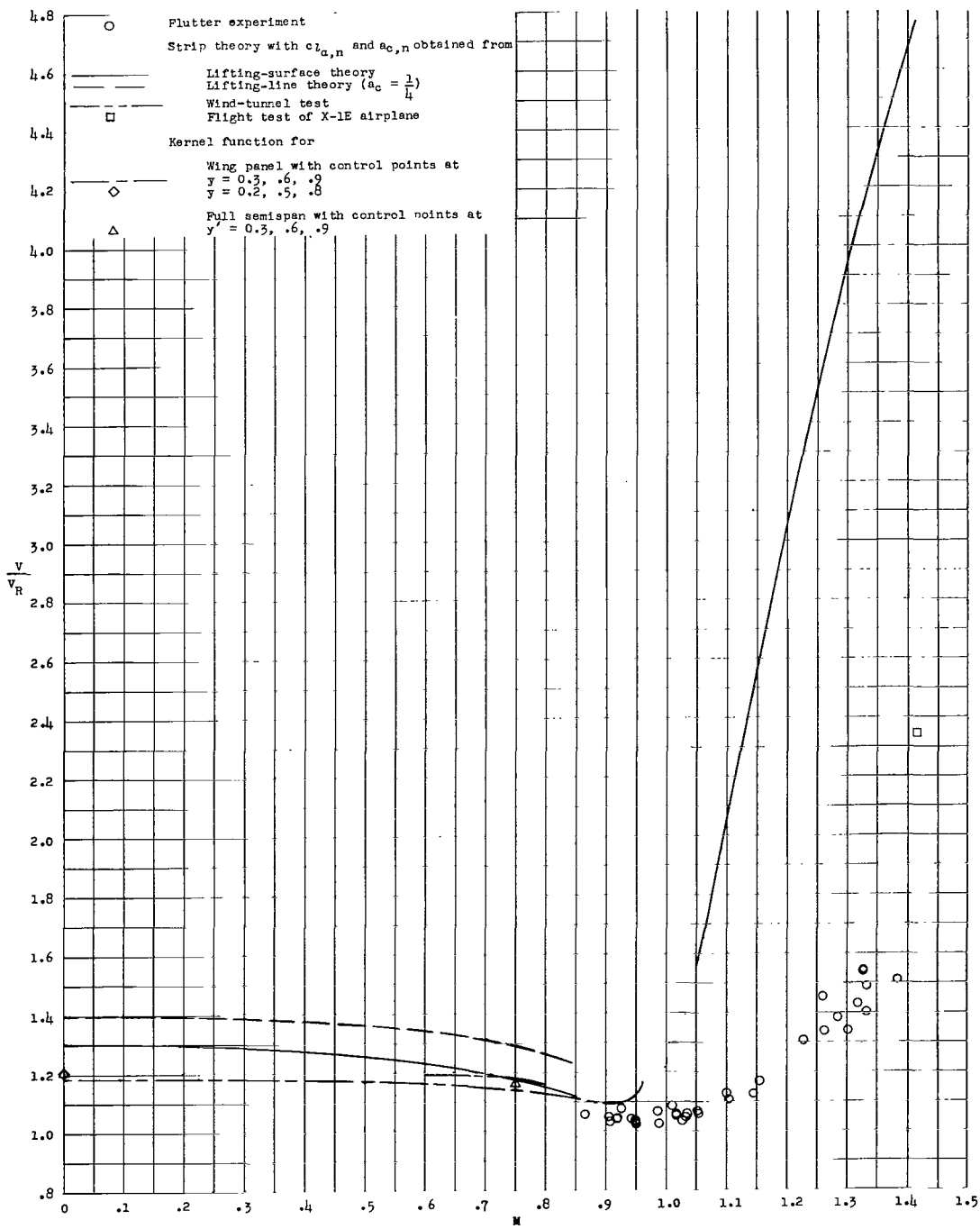

Figure 8.- Variation of flutter-speed ratio with Mach number for wing 400. For calculated points ρ = 0.002378 slug/cu ft and V_R = 976.5 ft/sec. Three uncoupled vibration modes were used in all calculations.

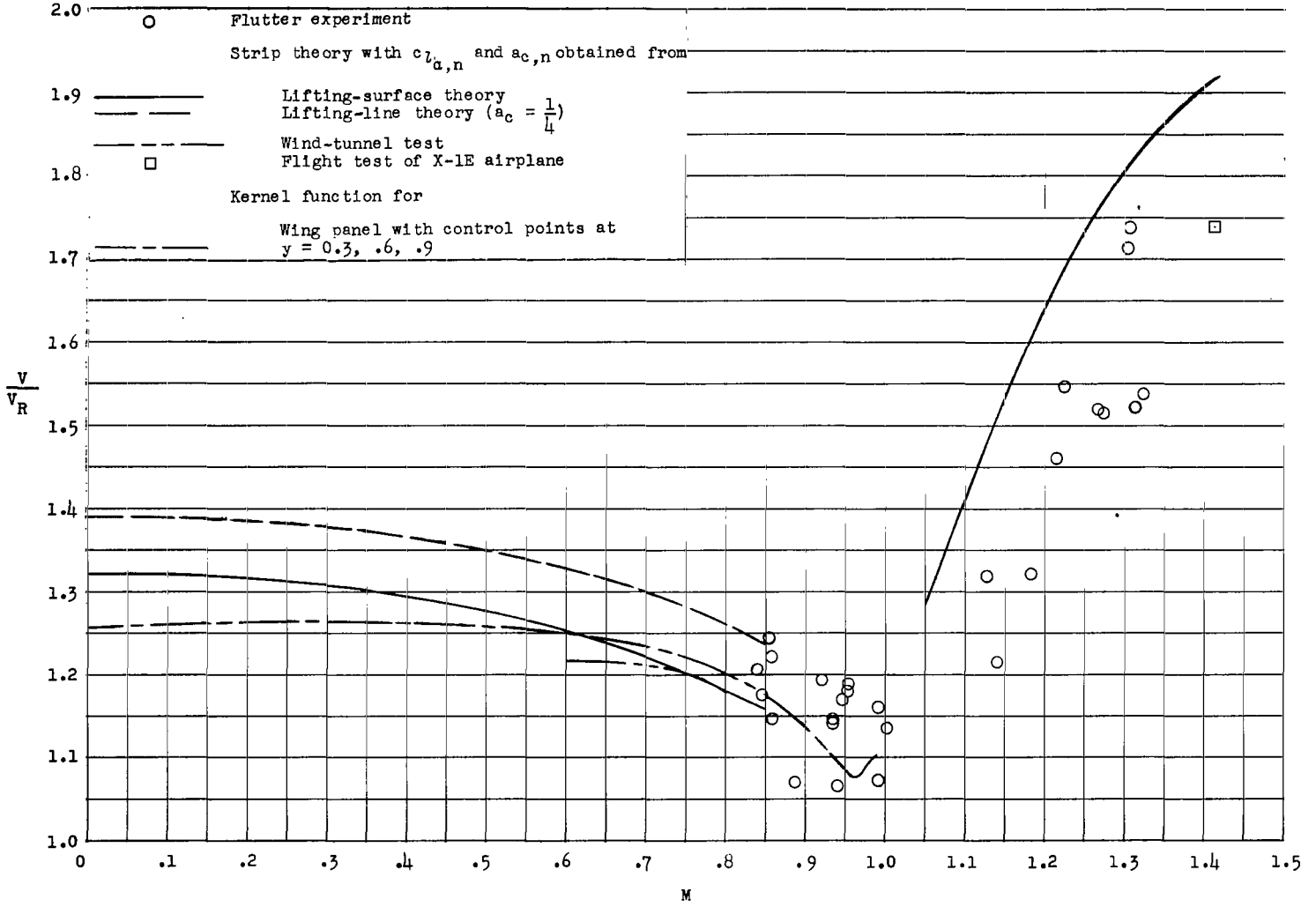

Figure 9.- Variation of flutter-speed ratio with Mach number for wing 400R. For calculated points $\rho = 0.003100$ slug/cu ft and $V_R = 852.5$ ft/sec. Three uncoupled vibration modes were used in all calculations.

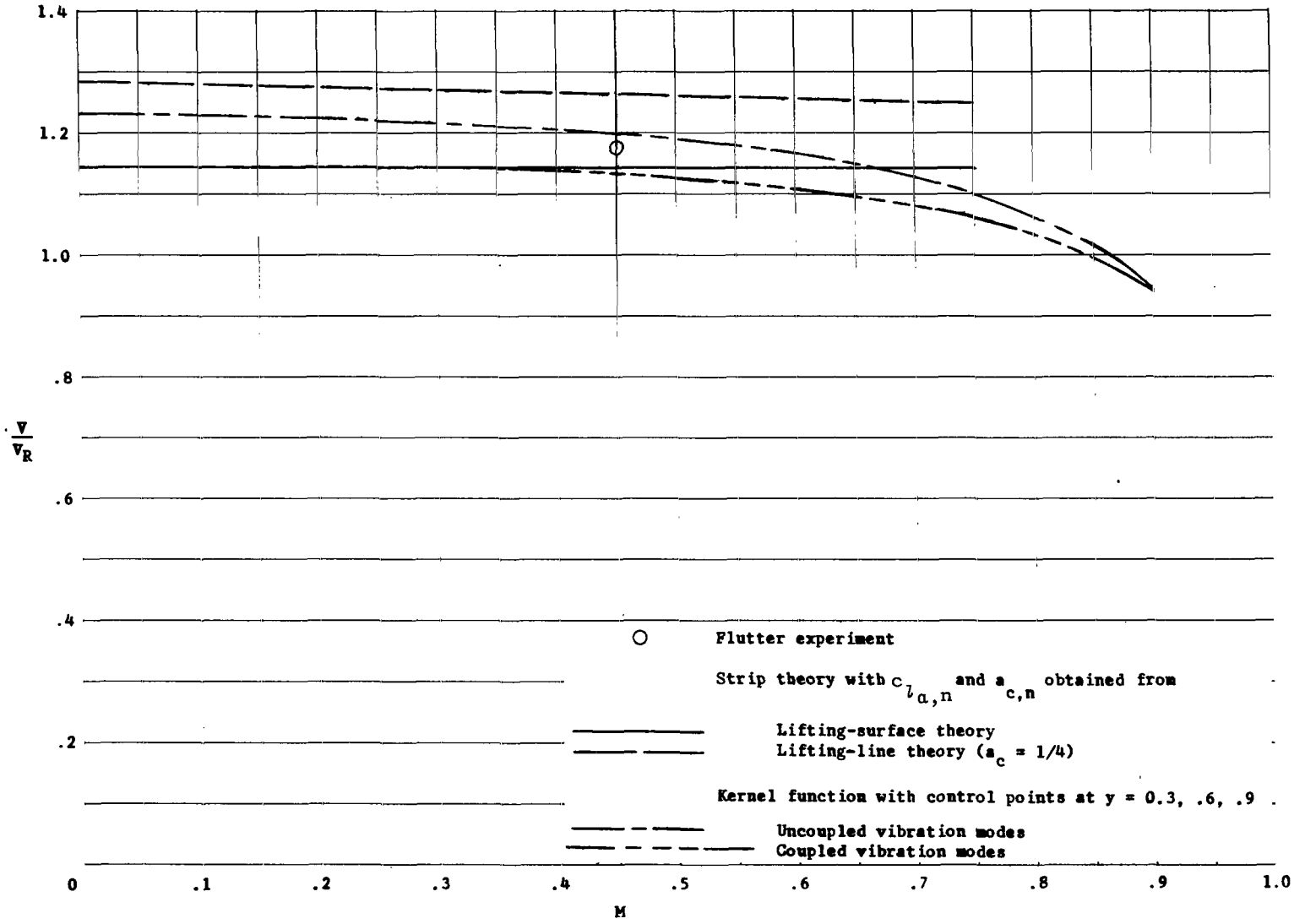

Figure 10.- Variation of flutter-speed ratio with Mach number for wing 5151. For all points ρ = 0.0023 slug/cu ft and V_R = 420.2 ft/sec. Three vibration modes were used in all calculations.

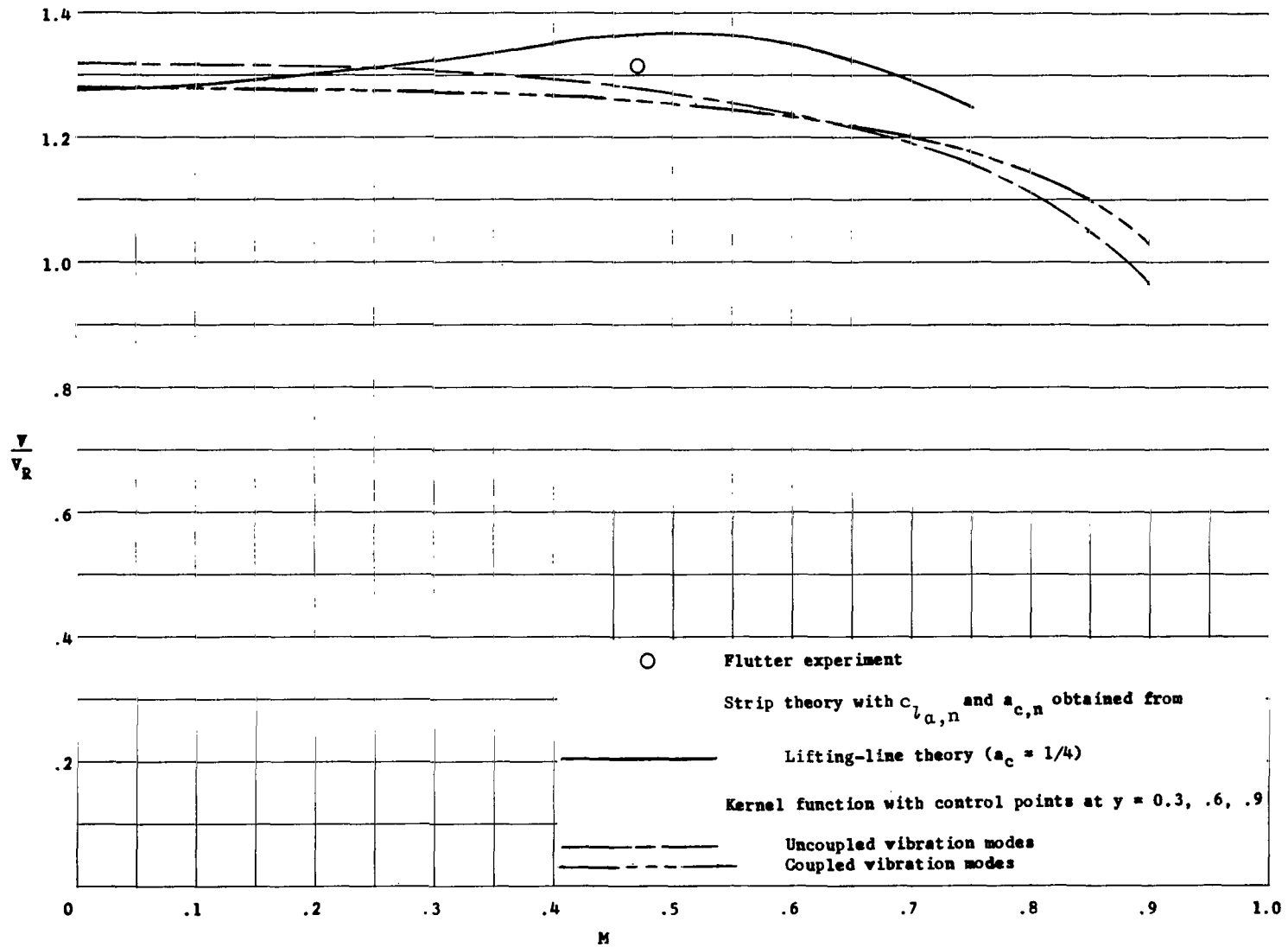

Figure 11.- Variation of flutter-speed ratio with Mach number for wing 4301. For all points ρ = 0.0023 slug/cu ft and V_R = 392.9 ft/sec. Three vibration modes were used in all calculations.

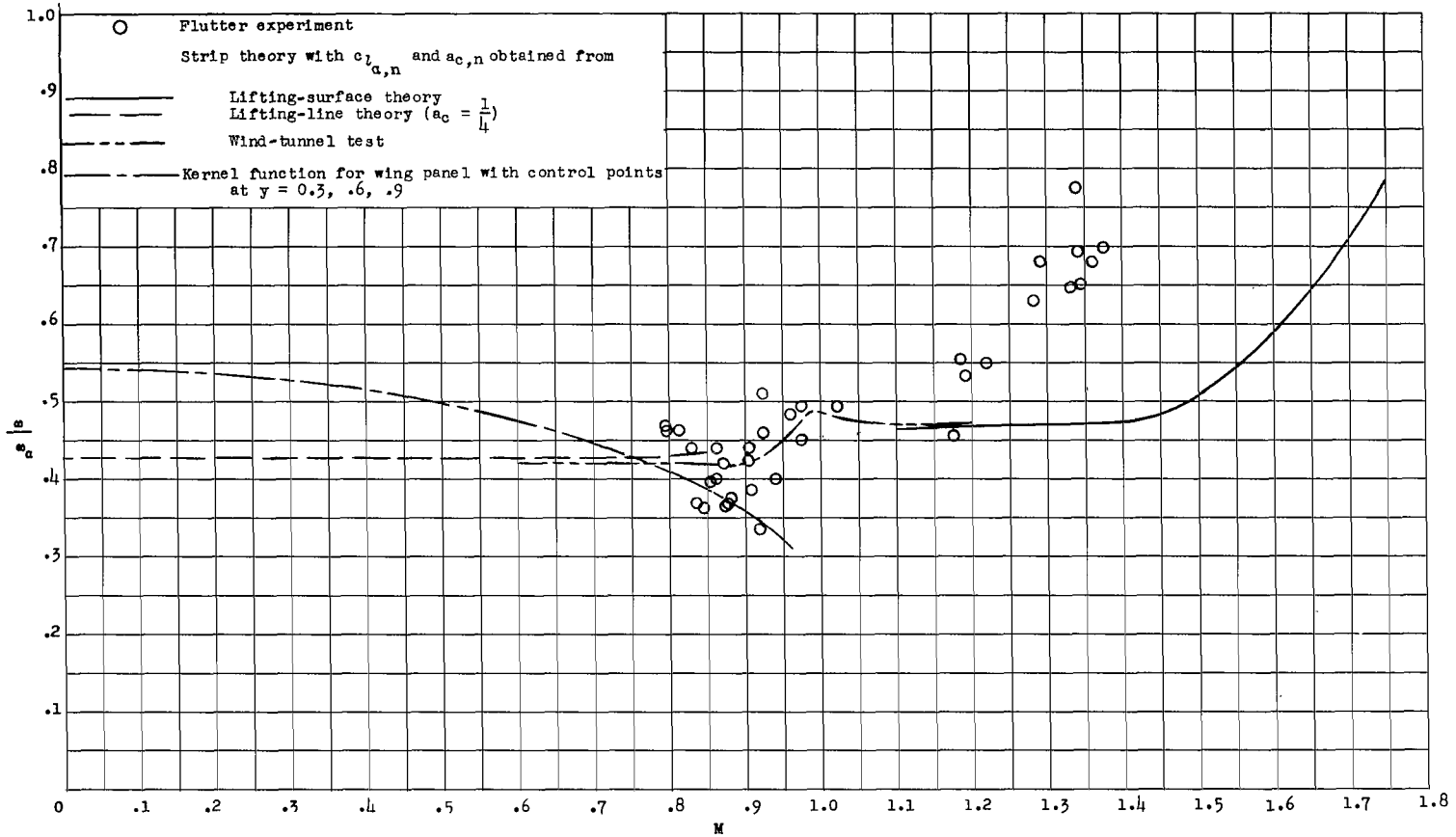

Figure 12.- Variation of flutter-frequency ratio with Mach number for wing 445. For calculated points ρ = 0.003800 slug/cu ft and ω_α = 2192 radians/sec. Three uncoupled vibration modes were used in all calculations.

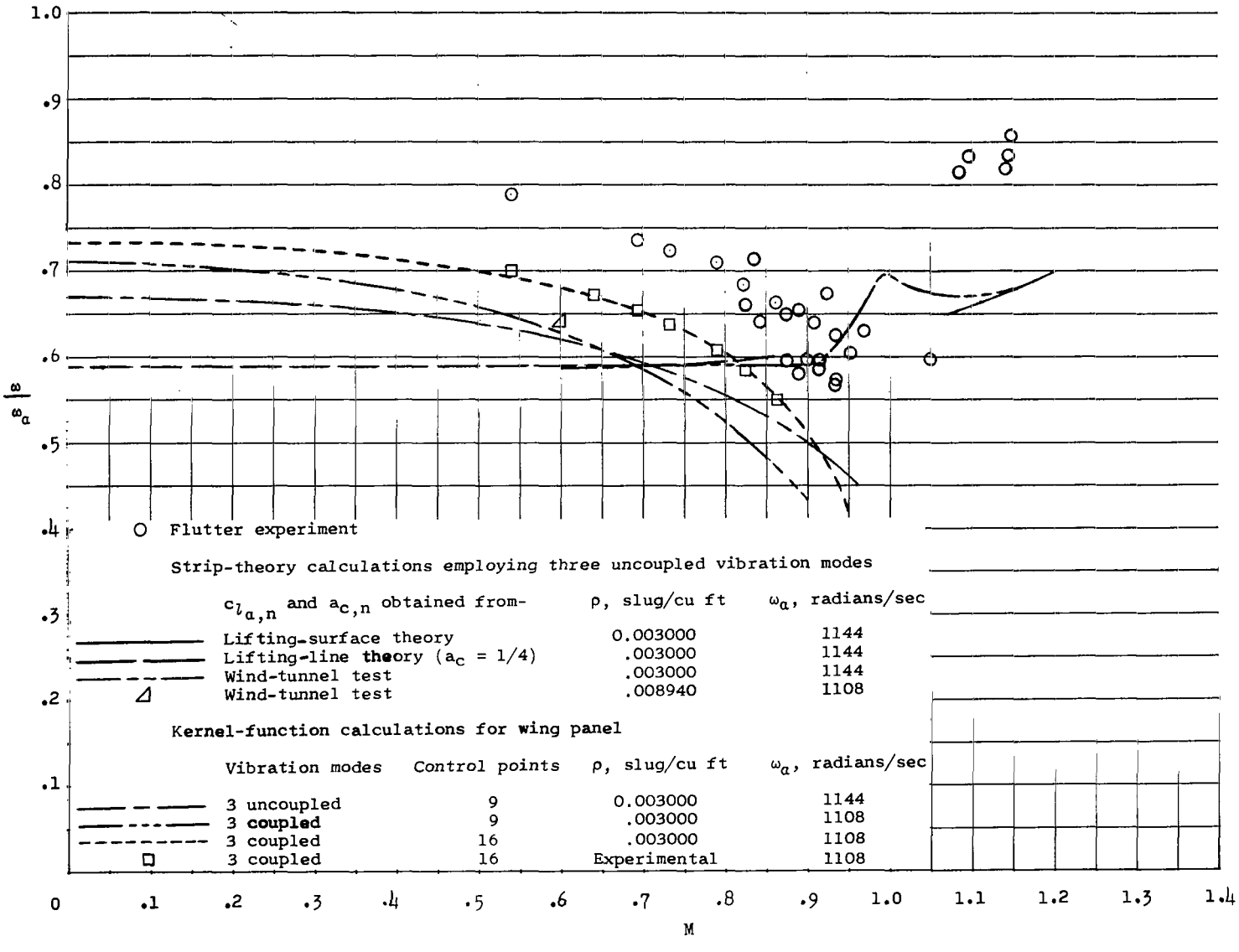

Figure 13.- Variation of flutter-frequency ratio with Mach number for wing 445F.

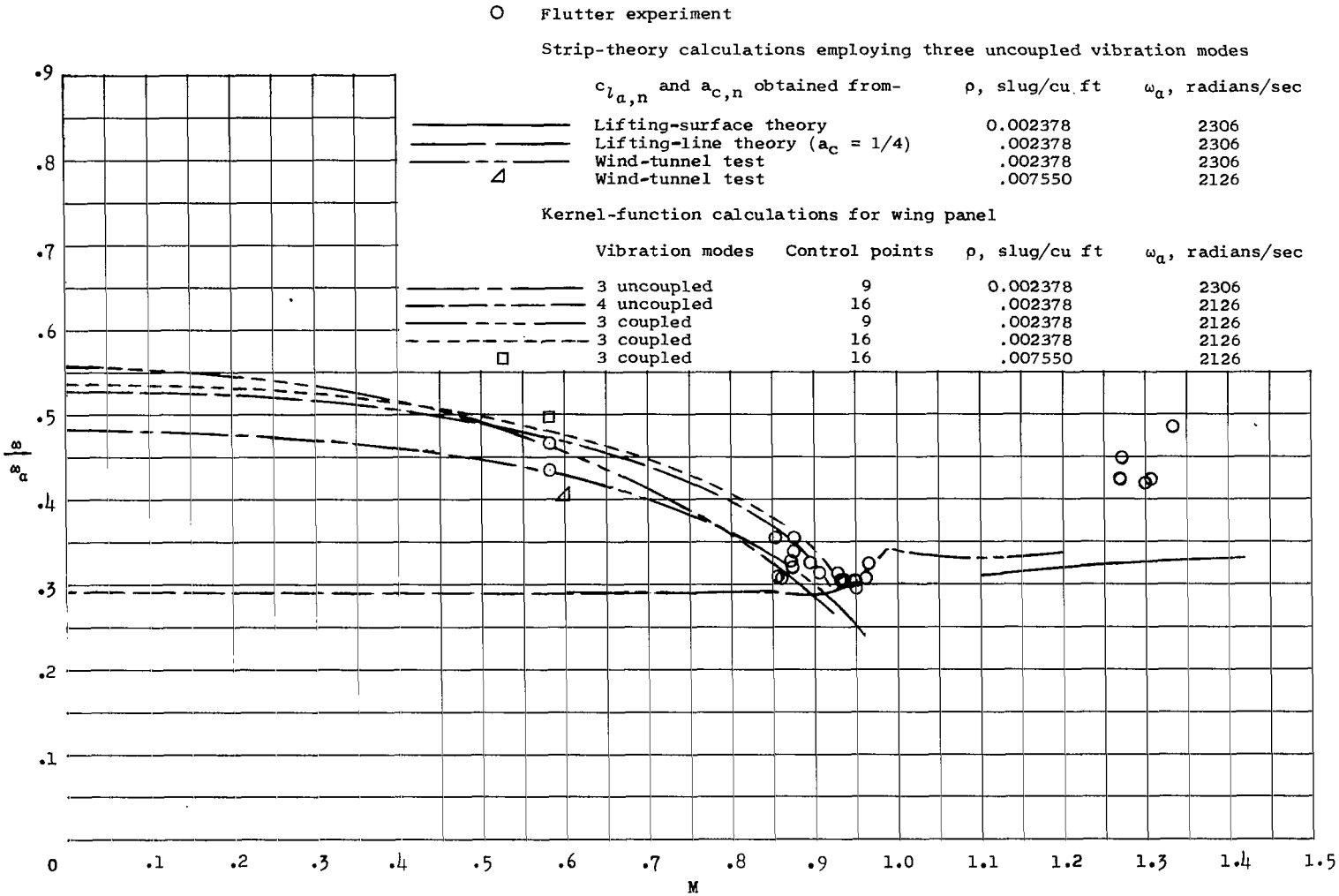

Figure 14.- Variation of flutter-frequency ratio with Mach number for wing 445R.

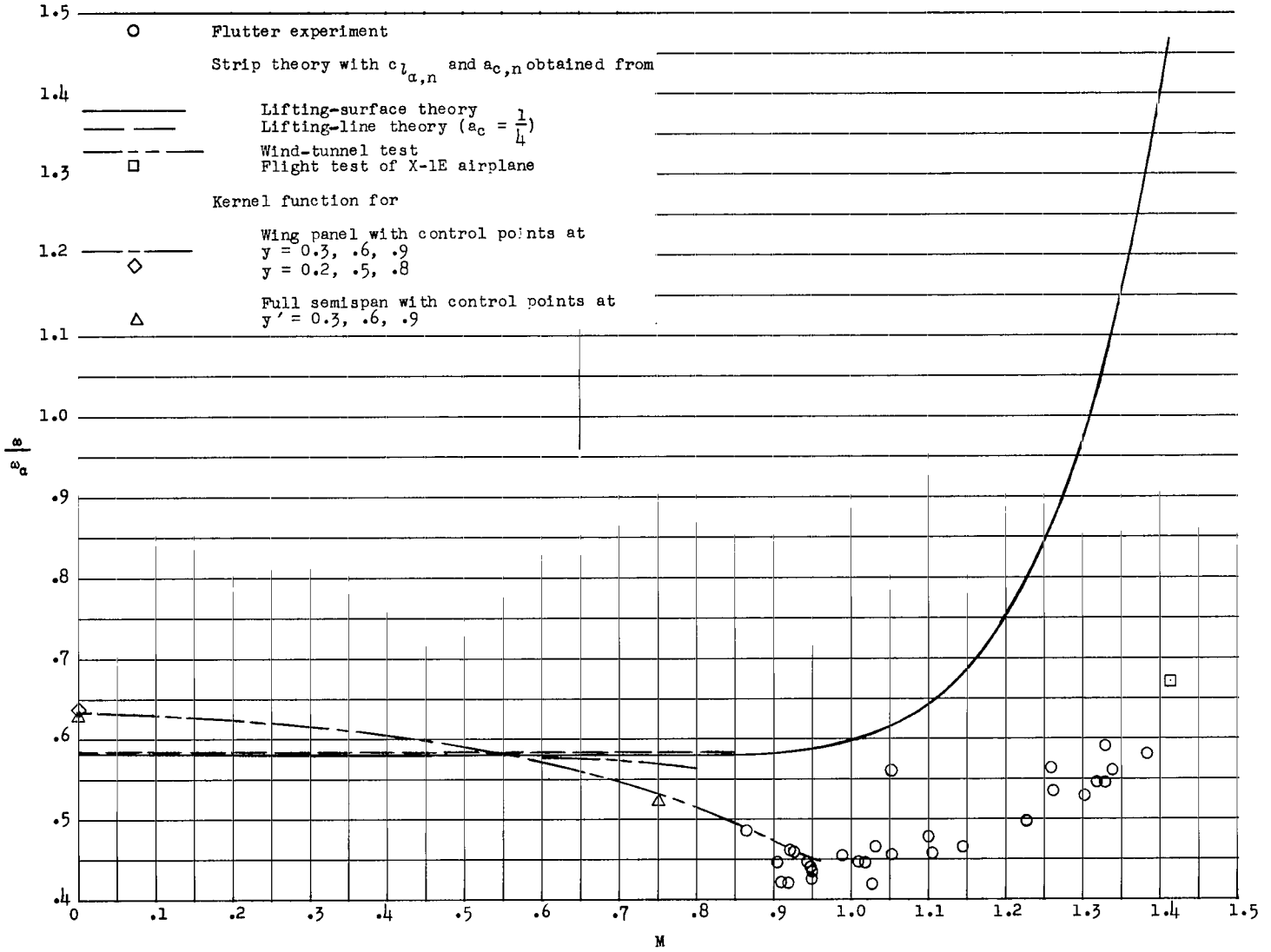

Figure 15.- Variation of flutter-frequency ratio with Mach number for wing 400. For calculated points ρ = 0.002378 slug/cu ft and ω_α = 2463 radians/sec. Three uncoupled vibration modes were used in all calculations.

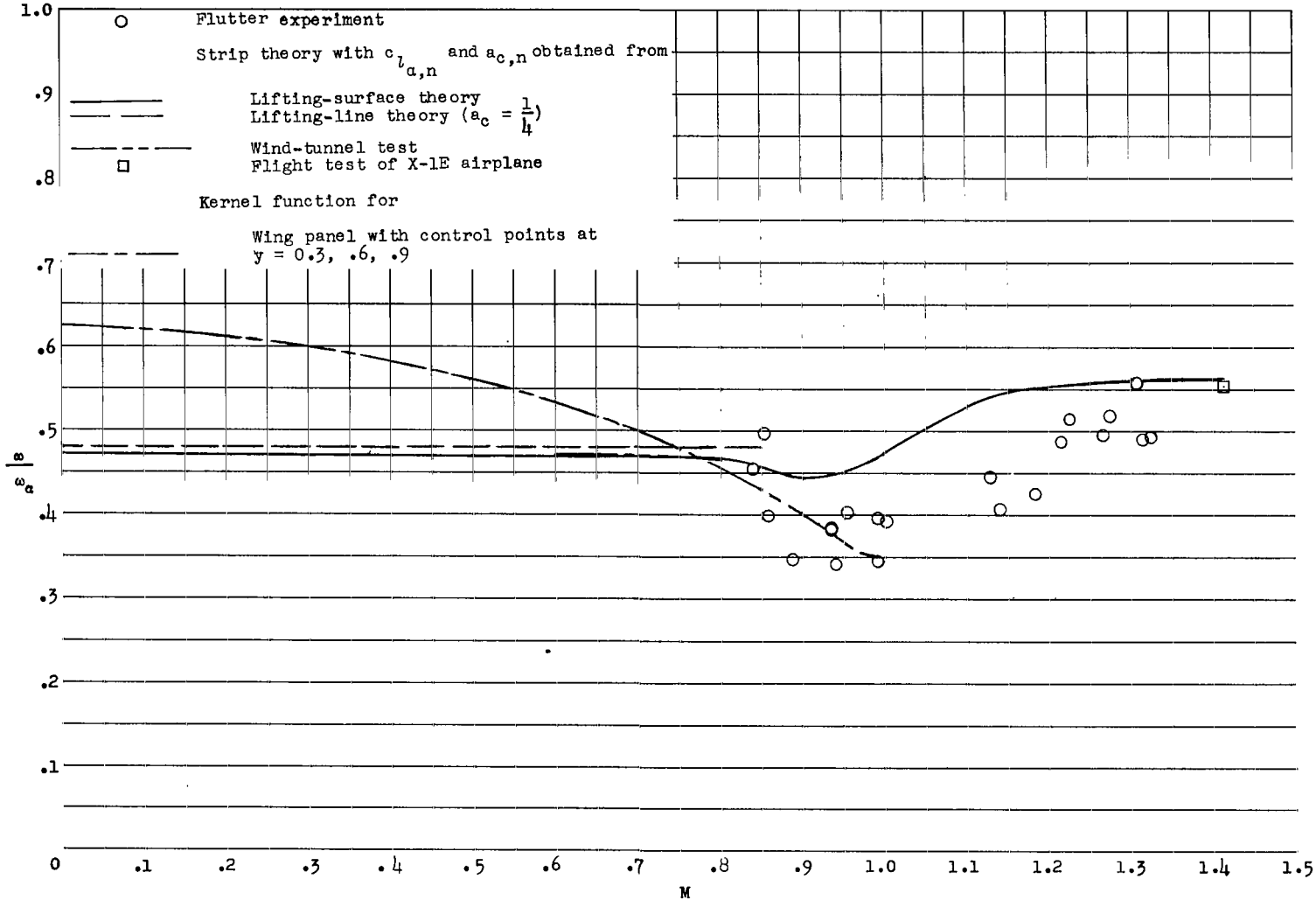

Figure 16.- Variation of flutter-frequency ratio with Mach number for wing 400R. For calculated points $\rho = 0.003100$ slug/cu ft and $\omega_\alpha = 1982$ radians/sec. Three uncoupled vibration modes were used in all calculations.

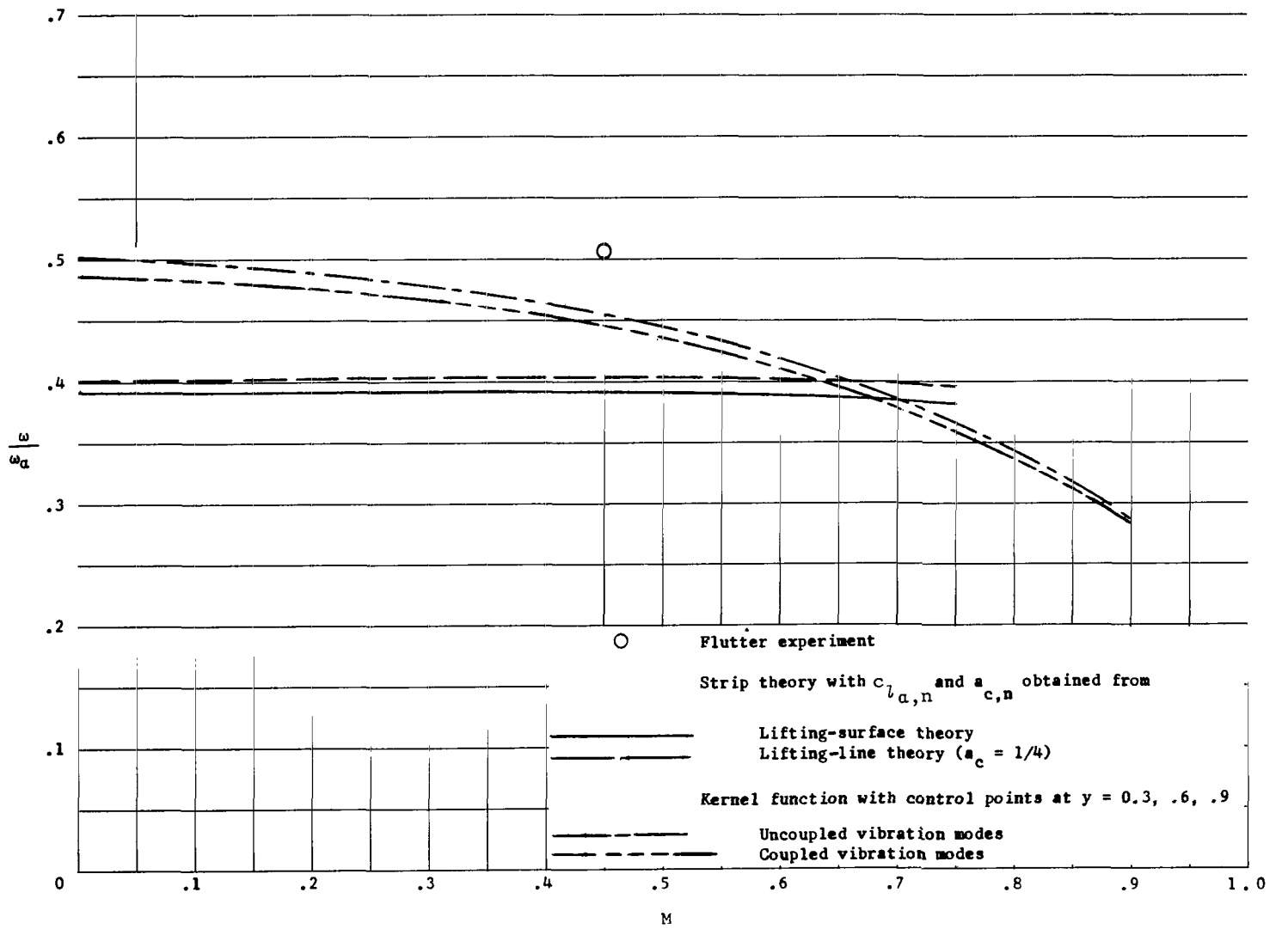

Figure 17.- Variation of flutter-frequency ratio with Mach number for wing 5151. For all points ρ = 0.0023 slug/cu ft and ω_α = 1488 radians/sec. Three vibration modes were used in all calculations.

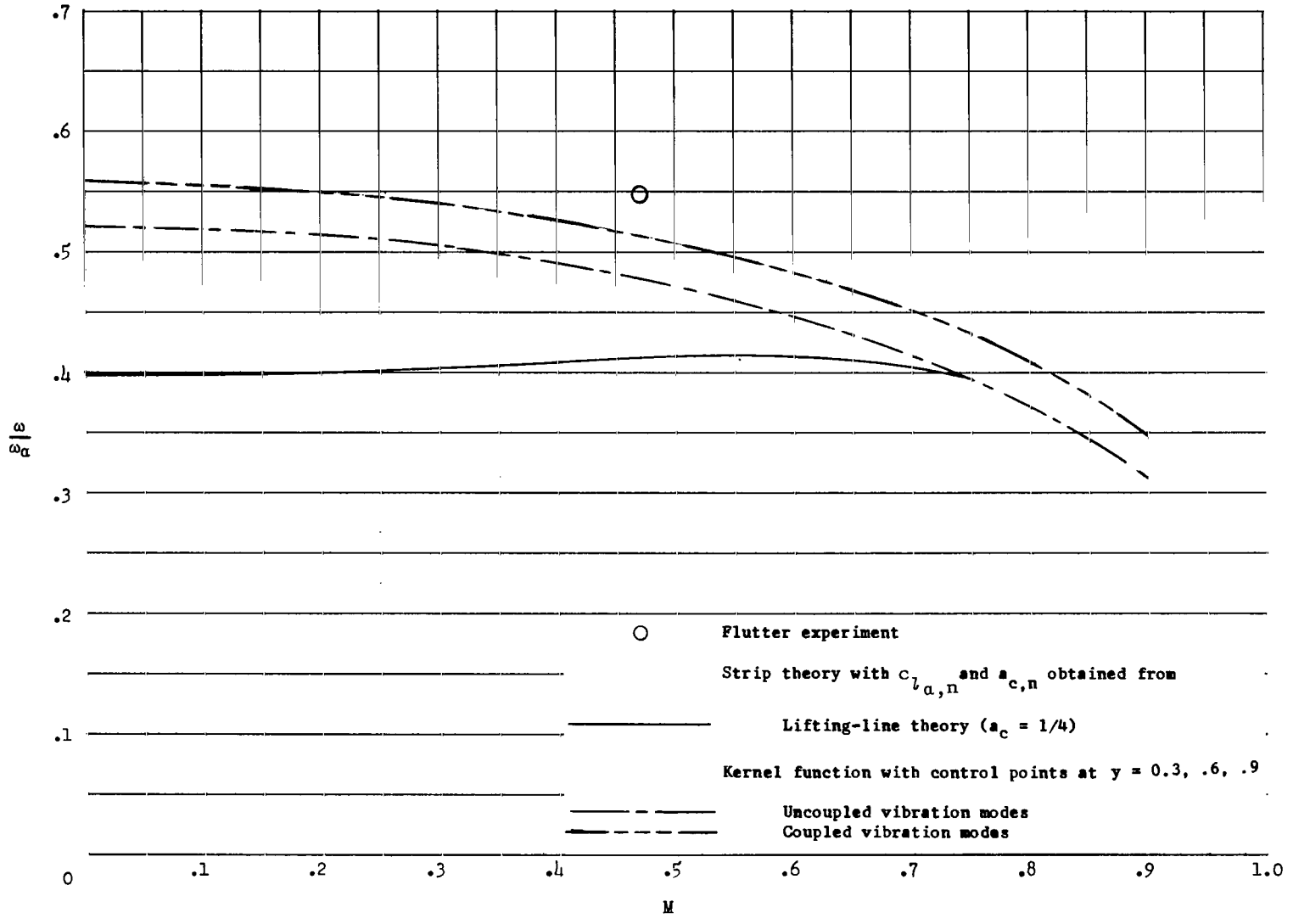

Figure 18.- Variation of flutter-frequency ratio with Mach number for wing 4301. For all points ρ = 0.0023 slug/cu ft and ω_α = 1376 radians/sec. Three vibration modes were used in all calculations.

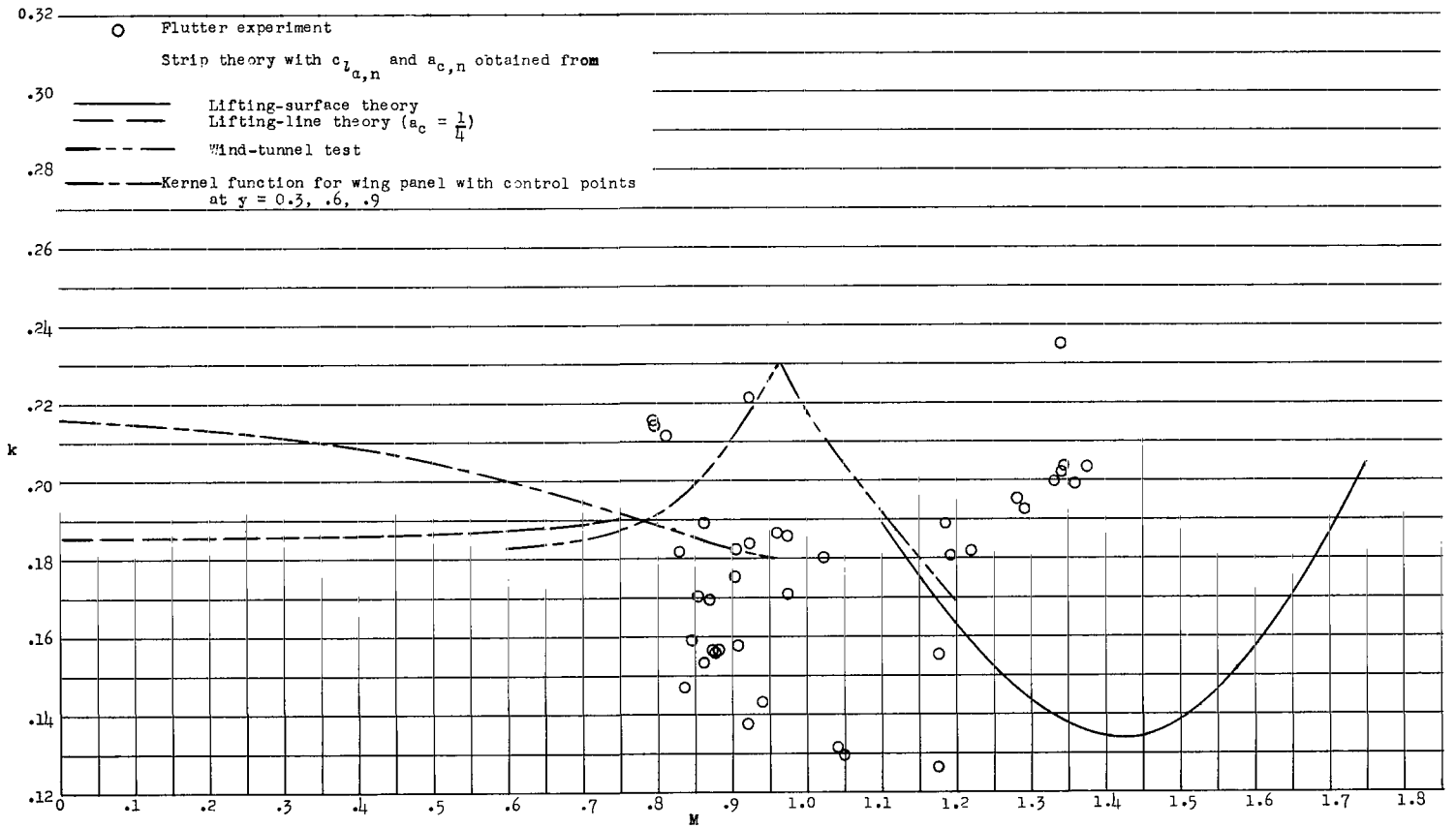

Figure 19.- Variation of flutter reduced frequency with Mach number for wing 445. For calculated points $\rho = 0.003800$ slug/cu ft. Three uncoupled vibration modes were used in all calculations.

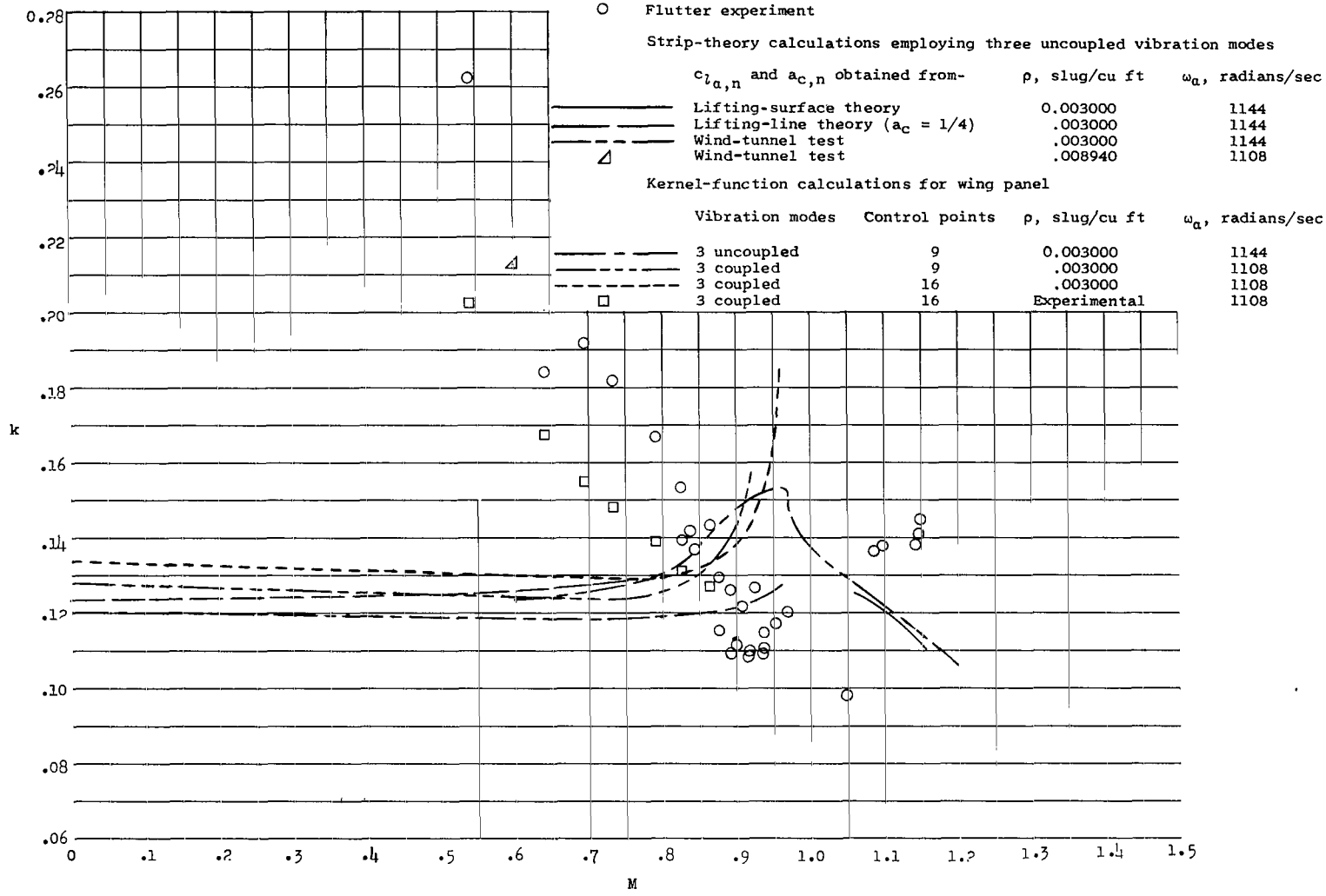

Figure 20.- Variation of flutter reduced frequency with Mach number for wing 445F.

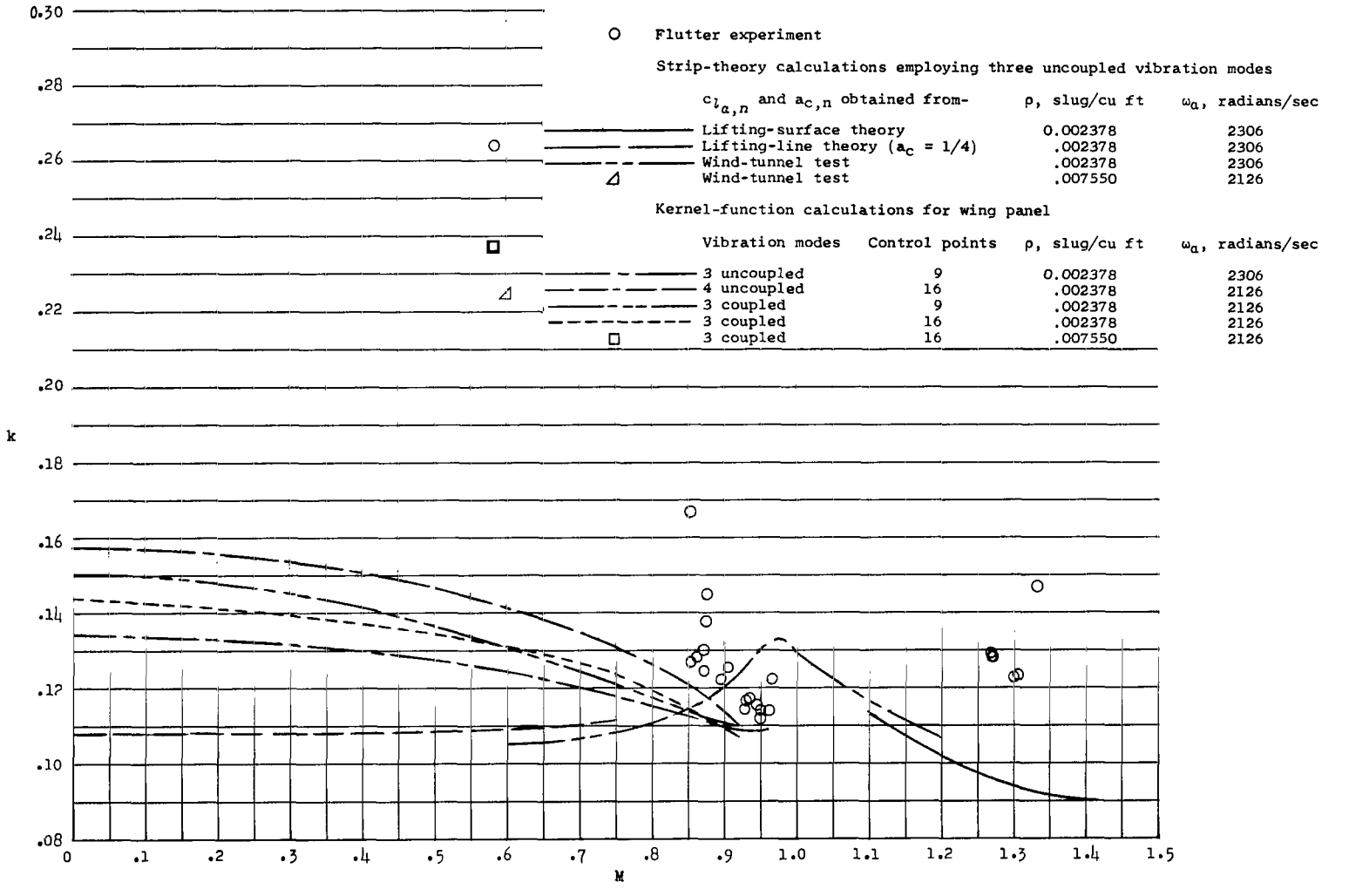

Figure 21.- Variation of flutter reduced frequency with Mach number for wing 445R.

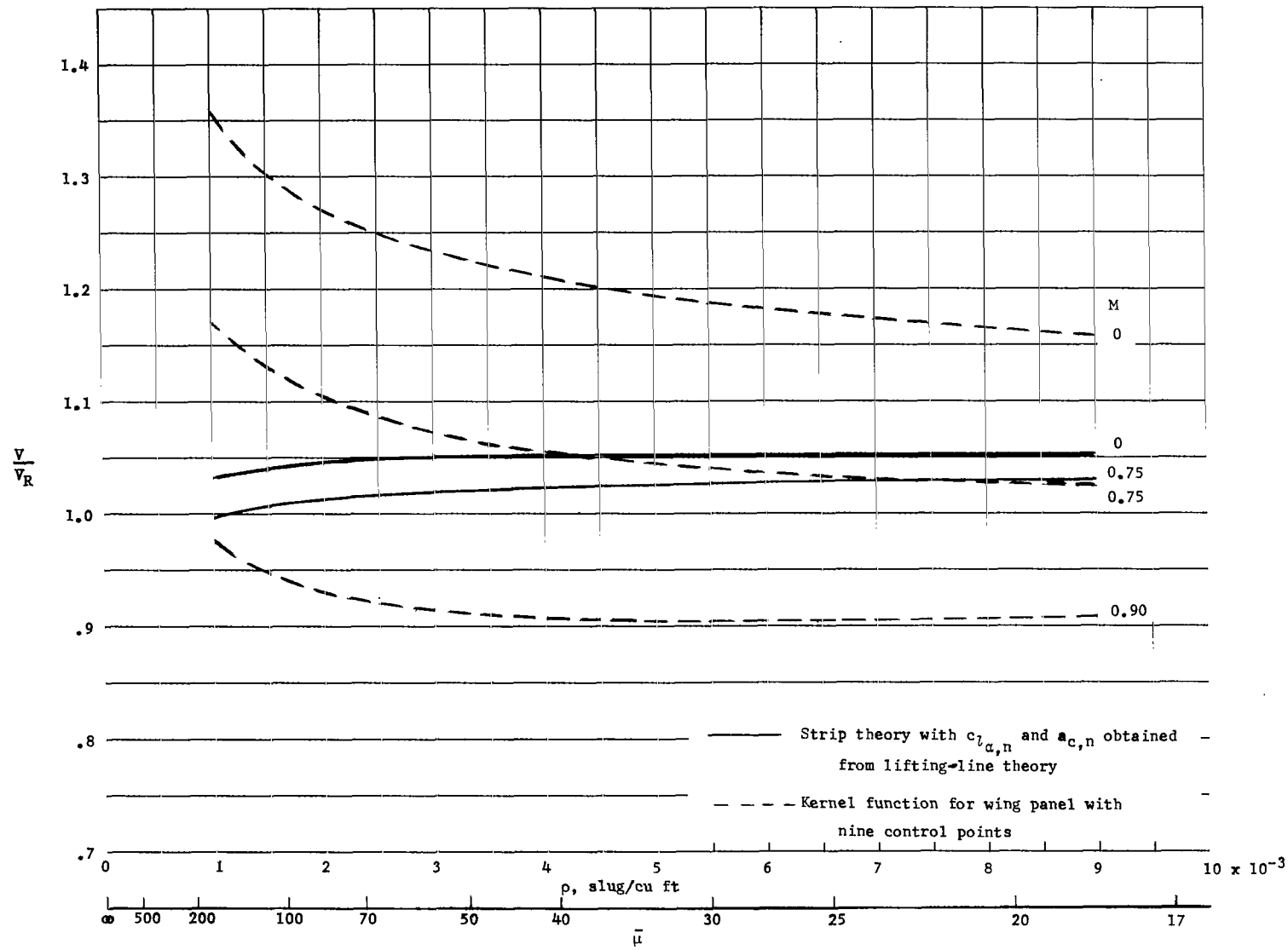

Figure 22.- Variation of calculated flutter-speed ratio with flow density for wing 445F. All calculations employ three uncoupled vibration modes.

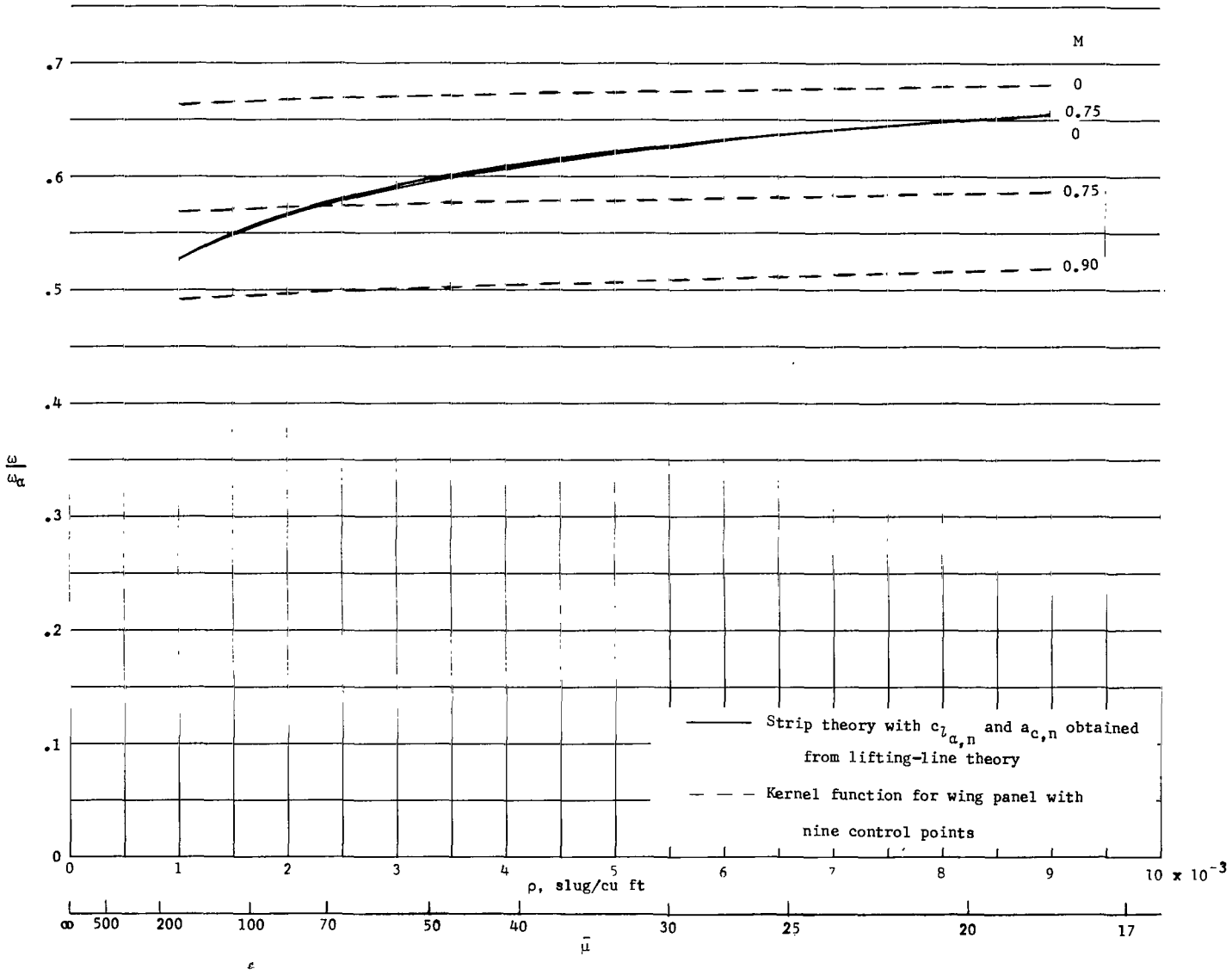

Figure 23.- Variation of calculated flutter-frequency ratio with flow density for wing 445F. All calculations employ three uncoupled vibration modes. ω_α = 1144 radians/sec.

"The National Aeronautics and Space Administration . . . shall . . . provide for the widest practical appropriate dissemination of information concerning its activities and the results thereof . . . objectives being the expansion of human knowledge of phenomena in the atmosphere and space."

—National Aeronautics and Space Act of 1958

NASA SCIENTIFIC AND TECHNICAL PUBLICATIONS

TECHNICAL REPORTS: Scientific and technical information considered important, complete, and a lasting contribution to existing knowledge.

TECHNICAL NOTES: Information less broad in scope but nevertheless of importance as a contribution to existing knowledge.

TECHNICAL MEMORANDUMS: Information receiving limited distribution because of preliminary data, security classification, or other reasons.

CONTRACTOR REPORTS: Technical information generated in connection with a NASA contract or grant and released under NASA auspices.

TECHNICAL TRANSLATIONS: Information published in a foreign language considered to merit NASA distribution in English.

TECHNICAL REPRINTS: Information derived from NASA activities and initially published in the form of journal articles or meeting papers.

SPECIAL PUBLICATIONS: Information derived from or of value to NASA activities but not necessarily reporting the results of individual NASA-programmed scientific efforts. Publications include conference proceedings, monographs, data compilations, handbooks, sourcebooks, and special bibliographies.

Details on the availability of these publications may be obtained from:

SCIENTIFIC AND TECHNICAL INFORMATION DIVISION

NATIONAL AERONAUTICS AND SPACE ADMINISTRATION

Washington, D.C. 20546